REPORT DOCUMENTATION PAGE

Form Approved
OMB No. 0704-0188

1. REPORT DATE *(DD-MM-YYYY)*	**2. REPORT TYPE**	**3. DATES COVERED** *(From - To)*
30/04/2011	Final Technical Report	01/04/2010-30/04/2011

4. TITLE AND SUBTITLE

Enhanced Computational Toolbox Including Multiquantum Vibration-Translation (VT) & Vibration-Electronic (VE) Exchanges, Dissociation and Radiation Effects
Deliverable 4
Final Technical Report

5a. CONTRACT NUMBER
GS04T09DBC0017

5b. GRANT NUMBER

5c. PROGRAM ELEMENT NUMBER

6. AUTHOR(S)
Mistree, Farrokh; Aliat, A.; Vedula, P.

5d. PROJECT NUMBER
BY09-012SP

5e. TASK NUMBER

5f. WORK UNIT NUMBER

7. PERFORMING ORGANIZATION NAME(S) AND ADDRESS(ES)
High Performance Technologies Inc.
11440 Commerce Park Drive
Suite 600
Reston, VA 20191

8. PERFORMING ORGANIZATION REPORT NUMBER
BY09-012SP-D4

9. SPONSORING / MONITORING AGENCY NAME(S) AND ADDRESS(ES)
Department of Defense
High Performance Computing Modernization Program Office
10501 Furnace Road
Suite 101
Lorton, VA 22079

10. SPONSOR/MONITOR'S ACRONYM(S)
HPCMP, PETTT

11. SPONSOR/MONITOR'S REPORT NUMBER(S)

12. DISTRIBUTION / AVAILABILITY STATEMENT
Distribution Statement A: Approved for public release: distribution unlimited.

13. SUPPLEMENTARY NOTES

14. ABSTRACT

This document is the Final Technical Report for the PETTT Special Project BY09-012SP, Enhanced Computational Toolbox Including Multiquantum Vibration-Translation (VT) & Vibration-Electronic (VE) Exchanges, Dissociation and Radiation Effects. This project involved producing a computational toolbox for implementation of master equation based on detailed state-to-state (STS) kinetics. A toolbox has been developed to account for Vibration-translation (VT), Vibration-Electronic (VE), radiative transitions and state specific dissociation, based on nitrogen molecules (and atoms). The deliverable is in a modular form which can be interfaced with other related codes at AFRL to improve their prediction capabilities for accurate design and analysis of hypersonic vehicle trajectories. Accurate simulation of space vehicle trajectories requires high fidelity computational tools capable of describing complex multiphysics and nonequilibrium phenomena (present in the flow fields) especially due to translational, rotational, vibrational, ionization, dissociation, recombination and radiative modes. This toolbox facilitates the users to investigate and identify the dominant physical/chemical/electronic/other mechanisms particular to a problem and rapidly implement and evaluate new models as required. Using operator splitting algorithms, separate code modules for treatment of flow and treatment of STS kinetics were created. The code module for treatment of state-to-state kinetics may also

15. SUBJECT TERMS

PETTT, HPC, HPCMP, Real gas, dissociation, Radiation effects, multiquantum energy exchanges, Master equation, State-to-sta

16. SECURITY CLASSIFICATION OF:			**17. LIMITATION OF ABSTRACT**	**18. NUMBER OF PAGES**	**19a. NAME OF RESPONSIBLE PERSON**
					Andrew Mark
a. REPORT	**b. ABSTRACT**	**c. THIS PAGE**	UU	65	**19b. TELEPHONE NUMBER** *(include area code)*
Unclassified	Unclassified	Unclassified			703-812-4453

High Performance Technologies Inc.
11440 Commerce Park Drive, Suite 600
Reston, VA 20191

Enhanced Computational Toolbox Including Multiquantum Vibration-Translation (VT) & Vibration-Electronic (VE) Exchanges, Dissociation and Radiation Effects

BY09-012SP
Deliverable 04

Final Technical Report

Submitted by
Farrokh Mistree, A. Aliat and P. Vedula
30 April 2011

for
User Productivity Enhancement, Technology Transfer, and Training (PETTT) Program

High Performance Computing Modernization Program (HPCMP)

Contract No.: GS04T09DBC0017

Government Users/Sponsors/Partners: Eswar Josyula (AFRL/RHQ)

TABLE OF CONTENTS

1 Enhanced Computational Toolbox

As specified in the SOW for BY09-012SP, a computational toolbox for implementation of master equation based on detailed state-to-state (STS) kinetics was to be delivered. A toolbox has been developed to account for Vibration-translation (VT), Vibration-Electronic (VE), radiative transitions and state specific dissociation, based on nitrogen molecules (and atoms). The deliverable is in a modular form which can be interfaced with other related codes at AFRL to improve their prediction capabilities for accurate design and analysis of hypersonic vehicle trajectories. Accurate simulation of space vehicle trajectories requires high fidelity computational tools capable of describing complex multiphysics and nonequilibrium phenomena (present in the flow fields) especially due to translational, rotational, vibrational, ionization, dissociation, recombination and radiative modes. This toolbox facilitates the users to investigate and identify the dominant physical/chemical/electronic/other mechanisms particular to a problem and rapidly implement and evaluate new models as required. Using operator splitting algorithms, separate code modules for treatment of flow and treatment of STS kinetics were created. The code module for treatment of state-to-state kinetics may also be used as a standalone code for study of spatially homogenous (or zero-dimensional) flows, for a range of flow parameters. The enhanced toolbox is the primary project deliverable.

Throughout the performance of this project there has been continuous collaboration and communication between Government sponsor Josyula and the OU team. Interim versions of the toolbox have been provided as capabilities have been implemented. Fundamental studies based on the computational toolbox were presented in references [1, 2, 4, 5]. The delivery of the toolbox has been achieved via an OU maintained FTP site. The major capabilities of the enhanced toolbox include:

1.1 Effects of VT multiquantum energy exchanges

A simple model was proposed for computation of rate coefficients via accounting for multiquantum VT transitions based on the forced harmonic oscillator (FHO) theory. This model, which was developed by considering a quadrature method, provides rate coefficients that are in very good agreement with those found in the literature for the high temperature regime. It may be noted that the computational cost involved in obtaining the rate coefficients from our computational toolbox is much less than analogous approaches (e.g. quasi-classical trajectory (QCT)) available in the literature, and hence our toolbox can be efficiently integrated into relevant computational fluid dynamics codes (CFD).

This model was implemented in the toolbox and was later used to study (in a steady-state) a 1D inviscid N_2 gas flow through a plane shock (1D application) [1] and a blunt body (2D application) [2] by considering a STS approach. Although most studies in the literature are limited to VT monoquantum energy exchanges, our results (in 1D and 2D applications) show that VT multiquantum exchanges have a significant effect on the evolution of macroscopic gas parameters, and hence must be considered in predictive simulations of hypersonic flows in the high temperature regime. It may be noted that VT multiquantum (compared to monoquantum) transitions affect the populations of all vibrational levels, and the effective number of transitions decreases inversely according

to the vibrational quantum number. More details on the development of our VT model with results of its application can be found in references [1] (and also in Appendix A) and [2].

In the toolbox code, the state-specific source terms related to physico-chemical and radiative processes are computed based on active compiler flags in the Makefile, which control the presence of effects due to VT multiquantum transitions, dissociation, VE transitions and radiation. Examples of compiler flags that enable these controls are given in the table below:

Compiler flags for activation	**Processes (species)**
AVJRATES	VT transitions (N_2 molecules on their ground electronic state)
AVJRATES, DISSOCIATION	VT transitions + Dissociation (N_2 molecules and N atoms on their ground electronic state)
AVJRATES, VERATES	VT transitions + VE transitions (N_2 molecules on their ground and excited electronic states)
AVJRATES, VERATES, DISSOCIATION	VT transitions + VE transitions + Dissociation (N_2 molecules and N atoms on their ground and excited electronic states)
AVJRATES, VERATES, RAD	VT transitions + VE transitions + Radiation (N_2 molecules and N atoms on their ground and excited electronic states)
AVJRATES, VERATES, DISSOCIATION, RAD	VT transitions + VE transitions + Dissociation + Radiation (N_2 molecules and N atoms on their ground and excited electronic states)

The source terms due to VT (monoquantum and multiquantum) transitions, dissociation, VE transitions and radiation are computed in the interface subroutine "avjsource" (according to the various compiler flags mentioned above). These source terms are computed via a function call in the driver program/subroutine as, "call avjsource (ttemp, popin, xlum, poprates, omlum)", where the arguments to the subroutine are described as:

- ttemp = Translational temperature – (input)
- popin = State-specific populations (kg/m^3) – (input)
- xlum = Band intensities ($W/m^2/sr$) – (input)
- poprates = State-specific source terms ($kg/m^3.s$) – (output)
- omlum = Radiative source terms ($W/m^3.sr$) – (output).

In pure VT modeling, the N_2 molecules remain on their ground electronic state $X^1\Sigma$ and are the single component in the flow mixture. The dimension of variables “popin” and “poprates” is thus equal to the total number of vibrational levels of the $X^1\Sigma$ state. Without

radiation modeling, the radiative variables (xlum, omlum) are set to zero. The VT mode is characterized by its number of jumps via the user-defined "ijump" variable into the "avjrates" module, i.e.:

- ijump =1 (VT monoquantum transitions are considered)
- ijump = 6 (6 VT multiquantum transitions are considered)
- ijump = total number of vibrational levels (all VT multiquantum transitions are considered).

It may be noted that the function call "call avjsource (ttemp, popin, xlum, poprates, omlum)" is particularly useful for evolving the populations of various quantum levels ("popin") and the band intensities ("xlum") , for any temperature ("ttemp"), via integration of a coupled (and generally stiff) system of ordinary differential equations, according to an operator splitting approach described in [2]. The source terms (constituting the right hand side terms of these differential equations) are evaluated in "poprates" (corresponding to population in quantum levels) and "omlum" (corresponding to band intensities). Integration of such a stiff system of differential equations can be carried out using packages like LSODA/IVPAG available in ODEPACK/IMSL libraries. The interface module "avjrates" (containing the subroutine "avjsource") can be used to incorporate VT, VE, dissociation and radiation effects into other available CFD codes via state-to-state approaches.

1.2 Effects of the dissociation reaction

An efficient state-specific model of dissociation using a quadrature approach was proposed by considering the formalism of Macheret and Adamovich [3]. This formalism considers VT multiquantum transitions between bound (under the dissociation energy limit) and quasibound (over dissociation energy limit) vibrational levels. The dissociation model is based on the FHO theory to evaluate accurately the dissociation rates coefficients. The application of this model to a pure N_2 gas flow behind a plane shock wave shows that dissociation is preferential, i.e. it has a large influence on intermediate and higher vibrational levels. State-specific incubation distances are revealed and it appeared that VT energy exchanges remain the dominant mechanism just behind the shock. This last observation on VT transitions implies the need to account for multiquantum transitions (compared to those monoquantum commonly used in the literature) to correctly model the vibration-dissociation coupling.

More details on the development of our state-specific dissociation model with results of its application can be found in reference [4] and is given in appendix B.

As explained in the previous section, the toolbox already considers (by default) the VT transitions. The dissociation modeling is added via the "DISSOCIATION" flag into the Makefile. The dissociation of $N_2(X^1\Sigma)$ molecules lead to the production of nitrogen atoms on their ground electronic state ^4S. Therefore, the dimension of variables "popin" and "poprates" increases by one, by considering first the vibrational states of N_2 molecules. Without radiation modeling, the radiative variables (xlum, omlum) are set to zero.

1.3 Effects of VE exchanges and radiation

The VE energy exchanges occur between electronic states ($X^1\Sigma$, $A^3\Sigma$ and $B^3\Pi$) of N_2 molecules. The VE mechanisms are responsible for the formation of molecules on their electronically excited states ($A^3\Sigma$ and $B^3\Pi$). The VE model is implemented into the toolbox and its application for a one-dimensional shock-heated N_2 flow [1] shows that the concentration of excited molecules is weak. From this observation, the macroscopic gas parameters are mainly governed by the behavior of N_2 molecules on their ground electronic state. However, the VE modeling is necessary to evaluate the emitted radiation by the N_2 gas flow, because this radiation comes from radiative transitions between the excited electronic states as explained below.

The VE modeling is performed by using the "VERATES" flag into the Makefile. As VE transitions lead to the formation of N_2 molecules on their excited electronic states, the indices order of variables "popin" and "poprates" (of the "avjsource" subroutine) are first the vibrational states of $N_2(X^1\Sigma)$ molecules followed by those of $N_2(A^3\Sigma)$ and $N_2(B^3\Pi)$. The dissociation of these latter molecules leads to the formation of nitrogen atoms on their ground (^4S) and excited (^2D) electronic states, respectively. If VE transitions and dissociation are both modeled, the dimension of above variables increases by two by including the atomic electronic states (^4S and ^2D). Without radiation modeling, the radiative variables (xlum, omlum) are set to zero.

The radiative system implemented into the toolbox is the first positive system of N_2 molecules, i.e. from radiative transitions between the $A^3\Sigma$ and $B^3\Pi$ electronic states. The radiation model lies on the resolution of radiative transfer equations developed in a macroscopic scale to evaluate band intensities. This development takes into account of spectroscopic properties (fine structure, Hönl-London factors, Λ-doubling) and radiative mechanisms such as spontaneous emissions and induced emissions/absorptions. The radiation model is built in STS, commonly local thermodynamic equilibrium (LTE) and black body approaches. This model is implemented into the toolbox which is applied to study a one-dimensional shock-heated N_2 flow. Results show that the radiation emitted by the flow remains weak and is mainly comes from the spontaneous emissions. Due to this weak radiation, the STS and LTE approaches lead to similar intensities. Radiation effects are observed on the evolution of macroscopic gas parameters, as on the population of $N_2(B^3\Pi)$ due to their radiative de-excitations. The results also show that the coupling between the physico-chemical and radiative processes increases with the increase of the radiation intensity.

More details on the development of our VE and radiation models with results of their applications can be found in references [1] and [5] and given in appendixes A and C, respectively.

The radiation modeling is introduced via the "RAD" flag into the Makefile. In this case, the dimension of radiative variables "xlum" and "omlum" is equal to the number of radiative bands transitions of the first positive system.

1.4 Identification of dominant energy exchange processes (VV, VT, VE, dissociation and/or radiation) for specific problems

Using the toolbox, the dominant mechanisms in high temperature gas flows were identified in references [1, 2, 4, 5]. The vibrational energy exchanges are essential to be modeled in STS approach because they are dominant just behind the shock [3] and other processes (as the dissociation reaction) are directly coupled to the vibration mode [6]. At high temperature conditions, the Vibration-Vibration (VV) transitions play a minor role compared to those of VT and thus can be neglected in the modeling [7]. The VT multiquantum mechanism is more realistic than that of monoquantum case commonly used in the literature. We developed a VT model to obtain accurate rate coefficients (base on the FHO theory) by using a quadrature method (to reduce the computing cost) and which can be easily used in computational fluid dynamics (CFD) modeling.

The recombination of molecules plays a minor role compared to the dissociation at high temperatures [8]. The dissociation modeling is thus a crucial point for the correct solution of master equations. We developed a state-specific dissociation model from the formalism of Macheret and Adamovich [3]. This model is based on the FHO model and a quadrature method to obtain accurate rates with a low computing cost. This model can be easily implemented in CFD modeling and is realistic because it takes into account the preferential mode of the dissociation.

The VE transitions lead to the formation of molecules in their excited electronic states. Results of our applications show that most of the N_2 molecules remain in their ground electronic state and thus govern the evolution of the gas parameters. From this observation, the VE transitions can be neglected in the kinetic scheme if the excited electronic states do not undergo other processes as radiative mechanisms.

We developed a model to evaluate the radiation from the first positive system of N_2 molecules, i.e. the radiative transitions between $A^3\Sigma$ and $B^3\Pi$ electronic states (VE transitions are thus considered). Its application shows that the radiation has an influence on population of electronic states related to the radiative transitions. Moreover, the coupling between the physico-chemical and radiative processes, increases with the increase of the radiation intensity.

1.5 Simulation of blunt body and expanding nozzle flows

The present toolbox can be used to simulate nonequilibrium N_2 gas flows at high temperatures, i.e. over ~8000K. This toolbox was applied to study successfully a one-dimensional and a two-dimensional blunt body flows behind a shock wave in a STS approach. The VT, VE, dissociation and radiative processes are taken into account and can be modeled separately to study their influence on the macroscopic gas parameters. Species are described on their ground and excited quantum states, i.e. on their electronic and vibrational levels.

Studies of expanding nozzles flows lie in lower temperature conditions. For this case, we suggest using the VE, dissociation and the radiation models of the toolbox. The vibrational energy exchanges (i.e. the VT and VV transitions) can be implemented for the instance with the commonly Schwartz-Slawsky-Herzfeld (SSH) [9] models which are generalized for anharmonic oscillators in [10, 11].

1.6 Identification of the areas where further model reduction algorithms are most needed

While the importance of considering VT multiquantum jumps (using the toolbox) was noted in references [1,2], the need for consideration of a reduced number of multiquantum transitions (as opposed to the consideration of all possible multiquantum transitions) was also identified [1,2]. Such reduced order models are meant to significantly reduce computational costs involved, while ensuring reliability and accuracy of predictive simulations. For instance, it was noted in reference [2] that consideration of no more than 6 multiquantum VT jumps (as opposed to a maximum of 48) from any given level appeared to be sufficient to give reliable predictions in the case of blunt body hypersonic flows in the high temperature regime. The reduced number of multiquantum jumps needed for reliable predictions was also found to depend on the vibrational quantum number [1], and hence further model reduction algorithms that identify the minimum number of reduced jumps for each vibrational quantum number are needed for a broad range of flow configurations and conditions.

Another approach for model reduction is to formulate an approach to consider only the most effective levels (as opposed to all levels) that account for physicochemical and radiative processes or alternatively consider the best representation of source terms (in master equations) for any reduced order representation. The latter can be addressed via the theory of optimal prediction and may be explored in the future.

2 Software Acceptance Status

Dr. Josyula and the OU team have been closely collaborating and there has been a rich two way technical interchange that has resulted in the deliverable of a useful and unique software capability. The software has been installed on Hawk and Diamond. Eswar Josyula, the AFRL sponsor, contacted 30 April, confirmed that "It has been delivered as indicated."

3 References

[1] A. Aliat, P. Vedula, and E. Josyula, "Simple model for vibration-translation exchange at high temperatures: Effects of multiquantum transitions on the relaxation of a N2 gas flow behind a shock." *Physical Review E*, 83, 026308 (2011).

[2] E. Josyula, A. Aliat, and P. Vedula, "Multiquantum state-to-state transitions in hypersonic blunt body flows." 49th AIAA Aerospace Sciences Meeting including the New Horizons Forum and Aerospace Exposition (American Institute of Aeronautics and Astronautics, Orlando, FL, 2011), AIAA 2011-0532.

[3] S. Macheret and I. Adamovich, "Semiclassical modeling of state-specific dissociation rates in diatomic gases." *Journal of Chemical Physics*, 113, pp.7351-7361 (2000).

[4] A. Aliat, P. Vedula, and E. Josyula, "State-specific dissociation modeling with multiquantum vibration-translation transitions." *Physical Review E*, 83, 037301 (2011).

[5] A. Aliat, P. Vedula, and E. Josyula, "State-specific modeling of radiation in reactive nonequilibrium gas flows." *Physical Review E*, (2011) - *in revision*.

[6] J. W. Rich and C. E. Treanor, "Vibrational relaxation in gas-dynamic flows." *Annual Review of Fluid Mechanics,* 2, pp.355-396 (1970).

[7] I. Adamovich, S. Macheret, J. Rich, and C. Treanor, "Vibrational relaxation and dissociation behind shock waves. Part 1- Kinetic rate models." *AIAA Journal*, 33, pp.1064-1069 (1995).

[8] Y. Stupochenko, S. Losev, and A. Osipov, "Relaxation in Shock Waves." (Springer-Verlag, Berlin, 1967).

[9] R. Schwartz, Z. Slawsky, and K. Herzfeld, "Calculation of vibrational relaxation times in gases." *Journal of Chemical Physics,* 20, pp.1591-1599 (1952).

[10] B. Gordiets, A. Osipov, and L. Shelepin, "Kinetic Processes in Gases and Molecular Lasers." (Gordon and Breach Science Publishers, Amsterdam, 1988).

[11] K. N. C. Bray, "Vibrational relaxation of anharmonic oscillator molecules: relaxation under isothermal conditions." *Journal of Physics B: Atomic, Molecular and Optical Physics,* 1, pp.705-717 (1968).

Appendix A: Computational toolbox structure

The VT, VE, dissociation and radiative processes are implemented into the following toolbox (avjsource) which can be used to study nonequilibrium gas flow in the high temperature regime. Code snippets of the toolbox are given below to illustrate the code structure, input/output interfaces, and compiler flags (to include physico-chemical and radiative effects).

```
!=======================================

! Interface module for the computational toolbox

!=======================================

..........

!---------------------------------------------------------

module avjrates

!---------------------------------------------------------

..........

!---------------------------------------------------------

contains

!---------------------------------------------------------

..........

!---------------------------------------------------------

subroutine avjsource (ttemp, popin, xlum, poprates, omlum)

! Computes the source terms of the master equations, related to

! physico-chemical and radiative processes, based on a State-to-State approach

!---------------------------------------------------------

implicit none

real(kind=8), intent(in) :: ttemp

! ttemp = Translational temperature

real(kind=8), dimension(NTOTLEVELS+NAT), intent(in) :: popin

! popin = State-specific populations  (kg/m3)
```

```
real(kind=8), dimension(NRAYS), intent(in) :: xlum
! xlum = Band intensities (W/m2/sr)
real(kind=8), dimension(NTOTLEVELS+NAT),intent(out) :: poprates
! poprates = State-specific source terms (kg/m3/s)
real(kind=8), dimension(NRAYS),intent(out) :: omlum
! omlum = Radiative source terms (W/m3/sr)
..........
call ev(evk)
! Calculation of energy of vibrational quantum levels
..........
call fpartvib(evk,ttemp,qvib)
! Calculation of partition function of vibration
..........
! ---> VT PROCESSES
call fvt(k,i1,i2,ik,evk,xfact,ttemp,pvt)
! Calculation of VT thermal probabilities
..........
#ifdef DISSOCIATION
! ---> DISSOCIATION PROCESS
call fvt(k,i1,i2,ik,evk,xfact,ttemp,pvt)
! Calculation of VT thermal probabilities
..........
# else
# endif
..........
#ifdef VERATES
! ---> VE PROCESSES
call vemod(k,ik,ttemp,pve)
```

```
! Calculation of VE rates

••••••••••

# else

# endif

••••••••••

#ifdef RAD

! ---> RADIATION

! Calculation of radiative source terms

••••••••••

# else

# endif

!-------------------------------------------------------

end subroutine avjsource

!-------------------------------------------------------

••••••••••

!-------------------------------------------------------

subroutine fvt(k,i1,i2,ikk,evk,xfact,tu,xint)

! Calculation of VT thermal probabilities

!-------------------------------------------------------

implicit none

integer(4), intent(in) :: i1, i2, ikk, k

! i1 = Index of the initial vibrational state

! i2 = Index of the final vibrational state

! ikk = Index of the partner collision

! k =  Index of the molecule which undergoes the VT transition

real(kind=8), intent(out) :: xint

! xint = VT thermal probabilities

••••••••••
```

```
!---------------------------------------------------------
end subroutine fvt
!---------------------------------------------------------

••••••••••

!---------------------------------------------------------
subroutine vemod(kk,ikk,ttemp,pve)
! Calculation of VE rates
!---------------------------------------------------------
implicit none
integer(4), intent(in) :: kk,ikk
! kk = Index of the molecule which undergoes the VE transition
! ikk = Index of the partner collision
real(kind=8), intent(in) :: ttemp
! ttemp = Translation temperature (K)
real(kind=8), intent(out) :: pve
! VE thermal probability (m3/s)

••••••••••

!---------------------------------------------------------
end subroutine vemod
!---------------------------------------------------------

••••••••••

!---------------------------------------------------------
subroutine fpartvib(evk,ttemp,qqvib)
! Calculation of partition function of vibration
!---------------------------------------------------------
implicit none
real(kind=8), intent(in) :: evk(NMOL,0:NLEVELS+NQBMAX),ttemp
! evk = Energy of vibrational quantum levels (J)
```

```
! ttemp = Translational temperature (K)
real(kind=8), intent(out) :: qqvib(NMOL)
! qqvib = Partition functions of vibration
••••••••••
!---------------------------------------------------------
end subroutine fpartvib
!---------------------------------------------------------
••••••••••
!---------------------------------------------------------
 subroutine ev(evk)
! Calculation of energy of vibrational quantum levels
!---------------------------------------------------------
implicit none
real(kind=8), intent(out) :: evk(NMOL,0:NLEVELS+NQBMAX)
! evk = Energy of vibrational quantum levels (J)
••••••••••
!---------------------------------------------------------
end subroutine ev
!---------------------------------------------------------
••••••••••
!---------------------------------------------------------
end module avjrates
!---------------------------------------------------------
!=========================================
```

Appendix B: A simple model for Vibration-Translation exchange at high temperatures: effect of multiquantum transitions on the relaxation of a N2 gas flow behind a shock

A. Aliat[1*], P. Vedula[1*] and E. Josyula[2]

[1]School of Aerospace and Mechanical Engineering, University of Oklahoma, USA

[2]U.S. Air Force Research Laboratory, Wright-Patterson Air Force Base, Ohio 45433, USA

[*]Corresponding authors: azizaliat@ou.edu, pvedula@ou.edu

Abstract

In this paper a simple model is proposed for computation of rate coefficients related to Vibration-Translation transitions based on the forced harmonic oscillator theory. This model, which is developed by considering a quadrature method, provides rate coefficients that are in very good agreement with those found in the literature for the high temperature regime (>~10000K). This model is implemented to study a one-dimensional nonequilibrium inviscid N_2 flow behind a plane shock by considering a state-to-state approach. While the effects of ionization and chemical reactions are neglected in our study, our results show that multiquantum transitions have a great influence on the relaxation of the macroscopic parameters of the gas flow behind the shock, especially on vibrational distributions of high levels. All vibrational states are influenced by multiquantum processes, but the effective number of transitions decreases inversely according to the vibrational quantum number. For the initial conditions considered in this study, excited electronic states are found to be weakly populated and

can be neglected in modeling. Moreover, the computing time is considerably reduced with the model described in this paper compared to others found in the literature.

I. INTRODUCTION

Nonequilibrium vibrational kinetics at high temperature is a topic of interest in hypersonic aerodynamics studies [1]. One-temperature and multi-temperature models that are widely used in the literature to simulate hypersonic gas flows are based on the assumption of quasi-stationary distributions (Boltzmann or Treanor) over vibrational energies [2-5]. These quasi-stationary distributions are valid if characteristic mean times related to Vibration-Translation (VT), Vibration-Vibration (VV) and chemical reactions differ by many orders of magnitude. In particular, the one-temperature models assume significantly faster vibrational energy exchanges compared to chemical reactions, while multi-temperature models assume rapid VV and slow VT processes. However, more accurate rate coefficients calculated for VT, VV [6-10] and dissociation processes [10,11] show that their respective characteristic times are not very different from each other for a wide range of temperatures. Due to this observation, one-temperature and multi-temperature models can be deemed to be inadequate and hence more detailed state-to-state kinetic models are needed.

The main advantage of the state-to-state kinetic approach is that the population densities of vibrational quantum states are directly predicted, without the use of assumptions of any quasi-stationary distributions. Recently, many studies have been carried out with the state-to-state approach such as in high temperature N_2, O_2 and CO gas flows behind shock waves [12-17], expanding flows in nozzles [18-22], flows in boundary layers [23,24] and near blunt bodies [25-27]. Transport coefficients based on state-to-state kinetics were developed in reference [28] and results show a significant influence of nonequilibrium vibrational distributions on the heat transfer. Radiative processes are also taken into account in reference [29] and numerical applications [16,17] have shown evidence of the strong coupling between the physico-chemical and radiative processes. This strong coupling leads to the conclusion that the common local thermal equilibrium (LTE) assumption often used to treat radiative mechanisms [30-32], can result in significant errors in the evaluation of the radiation and the radiative heat issued by gas flows. Also, it was shown that excited electronic states can strongly influence the evolution of the macroscopic parameters of the gas flow behind a shock [16,17].

Densities of vibrational levels are initially governed by source terms related to VV and VT collisions in master equations. However, it was shown that VV mechanisms can be neglected at high temperatures (over ~ 10000K) for N_2 and CO molecules [16,33] and hence VT are dominant in vibrational energy exchanges. In this study we focus on the effects of pure VT multiquantum transitions, while neglecting the effects of radiation, ionization, dissociation, recombination and other chemical reactions which will be systematically included in future studies. Although the latter effects are important at high temperatures, the strong dependence of their rates on the nonequilibrium vibrational population levels necessitates accurate modeling of vibrational energy exchanges. For instance, dissociation of diatomic molecules, which is significant at high temperatures, proceeds preferentially from vibrational levels close to the dissociation energy, so that the

vibrational nonequilibrium affects the dissociation rate. Dissociation and the vibrational relaxation are thus strongly coupled and hence accurate modeling of diatomic gases requires a careful description of vibrational nonequilibrium to determine the degree of dissociation in the flow field.

Modeling of state specific rate coefficients for vibrational energy exchanges is widely discussed in the literature. Although semi-classical calculations for three-dimensional collisions [6-8] and exact quantum approach [9,10] provide good accuracy, they remain nevertheless computationally very expensive. However, the above accurate calculations are often used to fit the parameters in approximate approaches [34-36] which are commonly used because of their simplicity and low computing time. The rate coefficients utilized in computational fluid usually depend only on translational temperature. The most popular model of vibrational energy exchanges is that of Schwartz, Slawsky and Herzfeld (SSH) [37], which is based on a semi-classical first-order perturbation theory (FOPT). This model is developed for a collinear binary collision characterized by an exponential repulsive potential interaction; its generalization for anharmonic oscillators is given in references [38,39]. However, it is known that the SSH model works rather well for low quantum vibrational levels but fails at high collision velocities, high quantum numbers and cannot be applied for multiquantum jumps. To avoid these limits of application, a more rigorous theoretical approach is proposed on the basis of a nonperturbative forced harmonic oscillator (FHO) [40-42] also assuming a collinear binary collision. The FHO approach takes into account the coupling of many vibrational states during a collision, which can be valid at high temperature conditions and for multiquantum transitions. Adamovich et al. [43] extended the FHO model by including the anharmonicity of molecules and a steric factor to take into account the noncollinear nature of collisions. The steric factor is obtained from interpolations of experimental measurements or more accurate calculations. However, the direct use of FHO analytical expressions leads to numerical singularities and VT transition probabilities greater than unity at high vibrational quantum numbers [44,45]. Nevertheless under such conditions, the analytical expressions for the VT rate coefficients can be obtained using the model proposed by Nikitin and Osipov [46]. This asymptotic model uses properties of Bessel functions and appears to be valid in a whole vibrational quantum numbers and a large range of temperature [16,17,43].

However, it should be noted that VT rate coefficients are obtained by averaging transition probabilities over relative collision velocities via a distribution function. This average calculation is required for each transition and each temperature which can lead to a great computing time to obtain rate coefficients in master equations. For this reason, assumption of monoquantum collisions is commonly used and molecules remain on their ground electronic states to limit the number of VT transitions. An analytical model which can provide satisfactory FHO rate coefficients with a similar computing time as the SSH model, could greatly facilitate and extend numerical applications of the state-to-state approach for modeling gas flows at high temperatures.

In this paper, we propose a model which approximates that of Nikitin et al. [46] by considering properties of Bessel functions. Then, a quadrature method is utilized to calculate FHO rate coefficients related to VT transitions with a shorter computing time. To bring out the advantages of the proposed approach, the rate coefficients of both

multiquantum and monoquantum transitions calculated on the basis of the approximate model and that of Nikitin et al. are implemented to study a one-dimensional nonequilibrium inviscid N_2 gas flow behind a plane shock. Numerical results obtained from these two models in the context of relaxation of the gas flow macroscopic parameters are discussed. The significance of multiquantum transitions on the vibrational nonequilibrium description is evaluated and the underlying effects are compared to those obtained based on the restricted assumption of monoquantum transitions, which is widely used in the literature. Finally, computing times consumed by considering various VT models are estimated and compared.

II. FHO MODELS

A VT transition can be described by the following process:

$$A_{\alpha,i} + M \leftrightarrow A_{\alpha,i'} + M\,, \tag{1}$$

where terms α and i correspond to the electronic and vibrational states of a diatomic molecule A, respectively. As the result of VT collisional interaction with its partner M (atom or molecule), the molecule A is found on a different vibrational level i'(≠ i).The gap of vibrational energy $\Delta\varepsilon$ involved during this vibrational jump is shared with the translational mode of the molecule and its collisional partner, that is why the above process is called a Vibration-Translation transition. In this study, both monoquantum $\left(\left|i-i'\right|=1\right)$and multiquantum $\left(\left|i-i'\right|>1\right)$ transitions are considered.

The FHO transition probability related to the mechanism Eq.(1) is derived by Adamovich et al. [43] and given by:

$$P_{ii'}^{VT}\left(v_0\right) = i!\,i'!\,\varepsilon^{i+i'}\exp\left(-\varepsilon\right)\left|\sum_{r=0}^{n}\frac{(-1)^r}{r!(i-r)!(i'-r)!}\frac{1}{\varepsilon^r}\right|^2, \tag{2}$$

where $n=\min\left(i,i'\right)$, and ε is the average number of quanta transmitted to the initially nonvibrating oscillator, such as:

$$\varepsilon\left(v_0\right) = \frac{4\pi^3\omega}{\alpha^2\mu h}\left(\frac{\tilde{m}\gamma}{\alpha}\right)^2\sinh^{-2}\left(\frac{\pi\omega}{\alpha\,\bar{v}}\right). \tag{3}$$

Terms $\omega\left(=2\pi\Delta\varepsilon/h\right)$ and h are the angular frequency and the Planck's constant, respectively. The symmetrized relative collision velocity $\bar{v}\left[=\left(v_0+v_0^{'}\right)/2\right]$ takes into account the detailed balance and the total energy conservation during the VT interaction. The final relative collision velocity $v_0^{'}$ is connected to the initial velocity v_0 $\left(v_0^{'}=\sqrt{v_0^2+2\Delta\varepsilon/\tilde{m}}\right)$. The expression Eq.(3) is obtained on the basis of the repulsive exponential interaction potential $V(r)\sim\exp\left(-\alpha r\right)$ and its mass parameters $\left(\tilde{m},\gamma\text{ and }\mu\right)$ are given in the reference [43]. Moreover, the expression Eq.(3) is multiplied by a steric factor S_{VT} to take into account the noncollinear nature of collisions and is considered to be an adjustable parameter. In this study, we adopt the value of 4/9 proposed by

Adamovich et al. [43] for N_2-N_2 collisional interactions. This value is obtained from matching the above FHO transition probabilities at relatively low velocities with more accurate probabilities of Billing et al. [6]. Indeed, the latter authors performed calculations for three-dimensional collisions with a more realistic intermolecular potential.

However, the transition probability Eq.(2) cannot be used for vibrational energy exchange at high vibrational levels. Indeed, factorial calculations cannot be done accurately since numerical singularities (overflows and underflows) appear for high vibrational levels and unphysical transition probabilities are obtained [44,45]. For the high states, the following asymptotic model of Nikitin and Osipov [46] is suggested:

$$P_{ii'}^{VT}(v_0) = J_s^2(x_s), \tag{4}$$

where $x_s(v_0) = 2\sqrt{n_s \varepsilon}$ is introduced to facilitate the notation in the next section of the paper. The term J_s represents the Bessel function of the first kind at the s^{th} order, while $s = |i - i'|$ and $n_s = \left[\max(i,i')!/\min(i,i')!\right]^{1/s}$.

The rate coefficients $k_{ii'}^{VT}$ are obtained by averaging transition probabilities $P_{ii'}^{VT}$ given by Eqs.(2) and (4) over initial relative velocities as follows:

$$k_{ii'}^{VT}(T) = Z_M^{coll}(T) \int_0^{\infty} f_M^{dist}(v_0, T)\, P_{ii'}^{VT}(v_0)\, dv_0\,, \tag{5}$$

where the one-dimensional Maxwellian speed distribution function and the gas-kinetic frequency are given by [47]:

$$f_M^{distr}(v_0, T) = \left(\frac{\tilde{m}}{kT}\right) v_0 \exp\left(-\frac{\tilde{m} v_0^2}{2kT}\right) \tag{6}$$

and

$$Z_M^{coll}(T) = \sigma \sqrt{\frac{8\pi kT}{\tilde{m}}}\,, \tag{7}$$

respectively. Note that the above two expressions depend on the translational temperature T and are related to the collision partner M. The term σ is the collision diameter where chemical species are considered as hard spheres.

It is obvious that the direct calculation of the integral in Eq.(5) over initial relative collision velocities can involve significant computational costs (i.e. time) in fluid dynamics simulations. Indeed, the integral is computed at each variation of temperature for each VT transition. The number of VT transitions is proportional to the number of vibrational levels and can be very high. In the next section an approximate model is proposed to obtain FHO the rate coefficients and reduce greatly the computing time. This model is based on a quadrature method and uses properties of Bessel functions.

III. APPROXIMATE FHO MODEL

The Bessel function $J_s(x_s)$ in Eq.(4) is an oscillatory function and can be evaluated by its asymptotic functions $J_{1,s}$ and $J_{2,s}$ [48]. The use of these two functions allows us to approximate arbitrarily the VT transition probability Eq.(4) of Nikitin et al. [46] in three ranges of application as follows:

$$P_{ii'}^{VT}(v_0) \sim \begin{cases} J_{1,s}^2(x_s) = \left[\dfrac{1}{s!}\left(\dfrac{x_s}{2}\right)^s\right]^2 & x_s \in [0, x_{1,s}] \\ J_{1,s}^2(x_{1,s}) = J_{2,s}^2(x_{2,s}) & x_s \in [x_{1,s}, x_{2,s}], \\ J_{2,s}^2(x_s) = \dfrac{2}{\pi\, x_s}\cos^2\left[x_s - (2s+1)\dfrac{\pi}{4}\right] & x_s \in [x_{2,s}, \infty) \end{cases} \quad (8)$$

The main advantage of the above formulation is that we can evaluate the characteristics of peaks described by the square of the Bessel's function in the Nikitin and Osipov expression Eq.(4). Indeed, by considering the kth peak, it is easy to see in $[x_{2,s}, \infty)$ that its central position $x_{2,s,k}$ and its height $h_{2,s,k}$ are given by :

$$x_{2,s,k} = (2s+1)\pi/4 + (k-1)\pi, \quad (9)$$

and

$$h_{2,s,k} = 2/(\pi\, x_{2,s,k}), \quad (10)$$

respectively. The component $x_{1,s}$ in Eq.(8) describes the position of $J_{1,s}$ when it reaches a magnitude equal to the height of the first peak located at its central position $x_{2,s,k=1}$, i.e. $J_{1,s}^2(x_{1,s}) = J_{2,s}^2(x_{2,s,k=1})$. Under this condition, the component $x_{1,s}$ is given by:

$$x_{1,s} = 2\left(\frac{2\,s!}{\pi(s+1/2)^{1/2}}\right) \quad (11)$$

while asymptotic functions $J_{1,s}$ and $J_{2,s}$ are directly linked in the $[x_{1,s}, x_{2,s}]$ range.

Figure 1 shows the transition probability related to the monoquantum process $N_2(X^1\Sigma, i=5) + N_2 \rightarrow N_2(X^1\Sigma, i'=4) + N_2$. Note that $X^1\Sigma$ corresponds to the ground electronic state of N_2 molecules and monoquantum transitions involve the Bessel function at the first order (s=1). In this figure, we can see that higher peaks (k>1) of the Nikitin and Osipov model Eq.(4) are well described by the approximate form Eq.(8) in $[x_{2,s=1}, \infty)$. We approximate the first peak (k=1) of Nikitin et al. model using asymptotic functions $J_{1,s=1}$ and $J_{2,s=1}$ (illustrated by dashed lines) on the left and right slopes (respectively) of the first peak, which are bridged using a constant (plateau) value in the central region $[x_{1,s}, x_{2,s}]$ of the peak. The constant value is chosen to correspond to the extremum of $J_{2,s=1}$ located at $x_{2,s=1}$.

The presence of the peaks allows us to split the integral in Eq.(5) and obtain the following expression:

$$k_{ii'}^{VT}(T) = Z_M^{coll}(T)\sum_k I_k \tag{12}$$

with,

$$I_k = \int_{\Delta v_k} f_{AM}^{distr}(v_0, T) P_{ii'}^{VT}(v_0)\, dv_0 \,, \tag{13}$$

and where the term Δv_k corresponds to the velocity range at the endpoints of the kth peak. Moreover, we can observe in Fig.(1) that the collisional distribution function covers more peaks (k>1) at higher temperatures (as at 50,000K). Note that since peaks are rather sharp, we can assume that the magnitude of the distribution function varies slowly within them. So, in the first approximation we can assume that this magnitude is constant and equal to that on the central velocity $v_{2,s,k}$ within each peak k; the central velocity along v_0-axis corresponds to the above central position $x_{2,s,k}$ along x_s-axis. The assumption of slow variation committed by the distribution function allows us to rewrite Eq.(13) as follows:

$$I_k \sim f_M^{distr}(v_{2,s,k}, T) \int_{\Delta v_k} P_{ii'}^{VT}(v_0)\, dv_0 \,, \tag{14}$$

where the integral bound on the Δv_k range is simply the calculation of the area related to the kth peak. The surface of this peak can be estimated by the method of "triangles" [49], i.e. by multiplying its height $h_{2,s,k}$ by its width at the half-height $\Delta v_k^{'}$. Thus, the relation Eq.(14) becomes:

$$I_k \sim f_M^{distr}(v_{2,s,k}, T) P_{ii'}^{VT}(v_{2,s,k}) \Delta v_k^{'}. \tag{15}$$

Finally, introducing the above relation in Eq.(12), we can estimate the general VT rate coefficients Eq.(5) by a quadrature method as follows:

$$k_{ii'}^{VT}(T) \sim Z_M^{coll}(T)\left[I_{k=1} + \sum_{k>1} f_M^{distr}(v_{2,s,k}, T) P_{i,f}^{VT}(v_{2,s,k}) \Delta v_k^{'} \right]. \tag{16}$$

However, Fig.1 shows that the first peak (k=1) is larger than the other and that the assumption of slow variation of the collisional distribution function within this peak is not justified, especially at lower temperatures (as at 10,000K). To maintain the goal of reducing computing time without loss of accuracy in calculations at high temperatures, we split in the first approximation the integral $I_{k=1}$ Eq.(13) over the three ranges of application of the approximate transition probability Eq.(8) as follows:

$$I_{k=1} = \int_{x_{0,1}}^{x_{1,s}} + \int_{x_{1,s}}^{x_{2,s}} + \int_{x_{2,s}}^{x_{0,2}} \sim \sum_{j=1}^{3} I_{k=1}^{(j)}, \tag{17}$$

where components $x_{0,1}(=0)$ and $x_{0,2}(=(2s+3)\pi/4)$ correspond to the position of the end points of the first peak (k=1). The various sub-integrals $I_{k=1}^{(j)}$ are also evaluated by assuming a constant value of the distribution function and using the triangle integral method, similarly to the relation Eq.(15). The constant values are taken to be those evaluated at the mid-points of the first interval $[x_{0,1}, x_{1,s}]$ and last interval $[x_{2,s}, x_{0,2}]$, while in the central region $[x_{1,s}, x_{2,s}]$ the constant value is taken to be maximum value of the distribution function located at $x_{1,s}$. It may be noted that the approximation of the distribution function in the central region can also be alternatively chosen to correspond to the mid-point value. However the error in the latter approximation was found to be much higher (perhaps due to the rapid decay of the distribution function) and hence this alternative is not used.

The rate coefficients related to VT monoquantum transitions $N_2(X^1\Sigma, i) + N_2 \rightarrow N_2(X^1\Sigma, i-1) + N_2$ at low (i=5) and higher (i=25) quantum numbers are shown in Fig.2. We can see that the asymptotic model of Nikitin [46] agrees well that of Adamovich [43] in a wide range of temperature and vibrational states. The approximate model Eq.(16) of this study underestimates VT rate coefficients at low temperatures due to the simple quadrature calculation on the first peak ($I_{k=1}$). However, results obtained with this model become in a very good agreement with those of FHO models from nearly 8000K. Indeed, we saw that the distribution function covers more peaks (k>1) at higher temperature, so quadrature calculations on these peaks are more accurate due to their narrowness. Fig.3 confirms that the rate coefficients of monoquantum VT transitions Eq.(16) developed in this study can be used for high temperatures and in the whole range of vibrational levels.

Figure 4 illustrates VT multiquantum and monoquantum rate coefficients from the 30th vibrational level to lower states i (=20,28,29) of the N_2 molecules on their ground electronic state $X^1\Sigma$. We can see that multiquantum jumps predicted by Adamovich et al. [43] are in a good agreement with those given by the model of Nikitin et al. [46], so that from now only this latter reference is considered for the comparison. The approximate model Eq.(16) developed in this study provides a very good agreement of the rate coefficients with those given by the FHO models for temperatures over ~8000K.

Note that multiquantum rate coefficients (i=20,28) become comparable to that of monoquantum (i=29) with rising the translational temperature. Hence, multiquantum processes cannot be ignored in high temperature conditions. However, large multiquantum transitions (i=20) are very unlikely to occur at lower temperature since collision energies are not high enough to permit large energy jumps. Nevertheless, we can see in Fig.4 that the rate coefficient multiquantum transition (i=28) is not far from that of monoquantum (i=20) at low temperature. Indeed, since the energy levels become closer to each other with rising vibrational quantum numbers, the vibrational jumps become easier at moderate and high vibrational levels. Therefore, we can expect from the Fig. 4 that the first vibrational levels are populated mainly by monoquantum transitions and thus the well-known SSH model [37] can be applied for these levels at low temperature.

III. APPLICATION AND DISCUSSION

Similarly to the works in references [15-17,29,44], we consider a state-to-state nonequilibrium reactive gas flow, on the basis of kinetic equations for distribution functions in the spatial and temporal coordinates $(\mathbf{r},t)$. The gas flow is under the following condition:

$$\tau_{el} \sim \tau_{RR} \sim \tau_{RT} << \tau_{VT} \sim \tau_{VE} \sim \vartheta, \tag{18}$$

where $\tau_{el}, \tau_{RR}, \tau_{RT}, \tau_{VT}$ and τ_{VE} are the characteristic mean times related to elastic, Rotation-Rotation (RR), Rotation-Translation (RT), Vibration-Translation (VT), Vibration-Electronic (VE) processes; ϑ is the mean time of variation of macroscopic parameters. The above condition is satisfied in a wide temperature range, in particular for high enthalpy and high temperature hypersonic flows [1]. Under this condition and using the modified Chapman-Enskog method [29,50,51], the zero-order distribution function of diatomic molecules is found to be in the following form:

$$f_{\alpha,i}^{(0)} = \left(\frac{m}{2\pi k T}\right)^{3/2} \frac{N_{\alpha,i} s_j^{\alpha i}}{Z_{\alpha,i}^{rot}} \exp\left(-\frac{m\, C^2}{2kT} - \frac{\varepsilon_j^{\alpha i}}{kT}\right), \tag{19}$$

where m and k are the mass of the molecule and the constant of Boltzmann, respectively. Terms $s_j^{\alpha i}$, $\varepsilon_j^{\alpha i}$ and $Z_{\alpha,i}^{rot}$ are the rotational statistical weight, the energy of the rotational level j and the rotational partition function, respectively. These terms are related to the electro-vibrational state (α,i) of number density $N_{\alpha,i}$. The peculiar velocity $\mathbf{C}$ is connected to the macroscopic velocity $\mathbf{v}$ of the gas flow. The molecular distribution Eq.(16) describes a local Maxwell-Boltzmann distribution over velocities and rotational energies at the gas temperature T. The non-equilibrium character of the gas flow is carried by the electro-vibrational density $N_{\alpha,i}$.

The molecular distribution function Eq.(19) is expressed in terms of macroscopic parameters, $N_{\alpha,i}(\mathbf{r},t)$, $\mathbf{v}(\mathbf{r},t)$ and $T(\mathbf{r},t)$ which form a reduced set of variable to provide a closed self-consistent gas flow description in the state-to-state approach. A system of governing equations for these variables was derived in the general form in references [15,29]. In the Euler approximation of a one-dimensional stationary gas flow behind a shock, this system of equations leads to the conservation equations, momentum and total energy coupled to the equations of state-to-state vibrational-electronic kinetics [16,17]:

$$\frac{d\left(vN_{\alpha,i}\right)}{dx} = R_{\alpha,i} \tag{20}$$

$$pv\frac{dv}{dx} + \frac{dP}{dx} = 0 \tag{21}$$

$$pv\frac{dU}{dx} + P\frac{dv}{dx} = 0, \tag{22}$$

respectively. Terms x, v, P and U are the distance from the shock front, the flow velocity in the x direction, the pressure, and the total internal energy per unit mass, respectively. The source term in Eq.(20) is expressed as a sum of several source terms related to various processes:

$$R_{\alpha,i} = R_{\alpha,i}^{VT} + R_{\alpha,i}^{VE}. \tag{23}$$

The source term related to VT transitions is given by:

$$R_{\alpha,i}^{VT} = \sum_{M} N_M \sum_{i' \neq i} \left(k_{\alpha,i'i}^{M} N_{\alpha i'} - k_{\alpha,ii'}^{M} N_{\alpha i} \right), \tag{24}$$

where the term N_M corresponds to the number density of the collisional partner M in process Eq.(1). Forward rate coefficients $k_{\alpha,ii'}^{M}$ are calculated from the general form Eq.(5) by considering various VT models discussed in this paper. The backwards rate coefficients $k_{\alpha,i'i}^{M}$ are obtained from the detailed balance at the thermal equilibrium.

A VE transition can be described as follows:

$$A_{\alpha,i} + M \leftrightarrow A_{\alpha',i'} + M \tag{25}$$

where the molecule A on its initial electronic state α is found on a final electronic state α'. The molecule is assumed to remain on its ground vibrational level of the corresponding electronic state (i= i'= 0). The source term associated to this VE transition is:

$$R_{\alpha,i}^{VE} = \sum_{M} N_M \sum_{\alpha' \neq \alpha} \left(k_{\alpha'}^{M} N_{\alpha' i'} - k_{\alpha}^{M} N_{\alpha i} \right), \tag{26}$$

where rate coefficients k_{α}^{M} and $k_{\alpha'}^{M}$ are expressed in the Arrhenius form from Losev et al. [52] for N_2 molecules.

We apply the governing equation Eqs.(20), (21) and (22) to study a pure N_2 gas flow behind a plane shock wave. The ground $X^1\Sigma$ and first excited electronic states $A^3\Sigma$ and $B^3\Pi$ of N_2 molecules are considered in the modeling. These excited electronic states come from the VE transitions as follows [52]:

$$N_2\left(X^1\Sigma\right) + M \leftrightarrow N_2\left(A^3\Sigma, B^3\Pi\right) + M \quad . \tag{27}$$

Coefficients of Dunham given in references [53,55] are taken into account to calculate vibrational energy levels of N_2 molecules on their various electronic states. These coefficients lead to 49, 31 and 29 total vibrational levels for $X^1\Sigma$, $A^3\Sigma$ and $B^3\Pi$ states, respectively. The free stream conditions are the same as in Ref. [56], i.e. a Mach of 19.83, a temperature of 300K and a pressure of 27Pa. Indeed, we expect in the future to complete the two-dimensional hypersonic blunt body N_2 gas flow simulations by Josyula et al. [56] using the analysis of results obtained in this paper.

Our N_2 gas flow is simulating under a 2 GHz quad-core Intel Xeon processor, by considering a geometric progression of ~80000 grids along the x-axis. Numerical calculations run until a distance of 10 cm behind the shock is reached. The stiff ordinary

differential equations Eqs.(20), (21) and (22) are integrated by using the Gear's method [57].

Figure 5 shows the vibrational distributions of molecules $N_2\left(X^1\Sigma, i\right)$ for various levels i (=1,20,30,40) as functions of the distance behind the shock. Compared to monoquantum transitions, those multiquantum lead to a much faster relaxation of high vibrational states. Indeed, multiquantum mechanisms are more efficient on high levels because of their proximity to each other which involves low gap of energy exchanges. Consideration of multiquantum processes decreases slightly the concentration of first vibrational states to more populate higher levels. Note that results obtained with the VT model of this study Eq.(16) are in a good agreement to those obtained with the model of Nikitin et al. [46]. However, we can see in Table 1 that with the approximate model the one-dimensional N_2 gas flow code runs ~82 and ~107 times faster in cases of multiquantum and monoquantum collisions, respectively.

Local vibrational temperatures of each level i are illustrated in Fig.6 and are defined as follows:

$$T_v^{\alpha}\left(i\right) = \frac{\left(\varepsilon_i^{\alpha} - \varepsilon_{i=0}^{\alpha}\right)}{k \ln\left(N_{\alpha,i} / N_{\alpha,i=0}\right)}, \tag{28}$$

where the term ε_i^{α} corresponds to the energy of the vibrational level i related to the electronic state α. This figure confirms faster relaxation of high levels by considering multiquantum jumps. Indeed, vibrational temperatures of these states increase more rapidly with the distance from the shock compared to those of lower levels. In the case of monoquantum jumps, the behavior of these vibrational temperatures is opposite. Indeed, vibrational temperatures of high levels increase slower compared to those of lower states, because monoquantum processes involves vibrational energy exchanges only between nearest neighbor vibrational levels. Clearly, molecules reach a vibrational state by jumping step by step from the lower levels, which leads necessarily to a slower relaxation of high levels in the case of monoquantum transitions. This kind of displacement through levels of vibration also explains the shift of the thermal equilibrium obtained with the various models of VT energy exchanges. Indeed, molecules need more VT collisions to reach a vibrational level on a characteristic time of observation, so these molecules reach the thermal equilibrium on a longer distance behind the shock than in the multiquantum case.

In this Figure 6, we can also see that the translational temperature decreases more rapidly with the distance when we take into account multiquantum processes. This behavior rises from the rapid release of energy from the translational mode to the vibrational one resulting in the population of higher vibrational levels and allowing them a fast relaxation. Note that from the evolution of the translational temperature with the distance behind the shock, we can see that multiquantum processes become active when intermediate levels become enough populated from the first levels. Indeed, molecules on these intermediate levels can easily jump to higher vibrational states since energy levels become closer to each other for higher vibrational quantum number, and multiquantum transitions are more efficient when energy gaps are small. Figure 6 also confirms the limits of application of one/multi-temperature models. Indeed, these models assume a

single vibrational temperature for all levels which is not the case in the figure as shown by the state-to-state approach.

Figure 7 illustrates the vibrational distribution as functions of the vibrational quantum number related to N_2 molecules on their ground electronic state. This figure is obtained by considering multiquantum and monoquantum processes for various distances behind the shock (0.01 and 0.03 cm). It is clear that multiquantum mechanisms populate more quickly intermediate and high levels, i.e. for i >~10. With the mutiquantum transition case, the last vibrational levels seem to follow a Boltzmann distribution with a common vibrational temperature. Indeed, this can be explained by the fact that energies of these last levels are so close (compared to lower levels) that few VT collisions permit them to follow a similar relaxation behind the shock. However, concentrations of the first levels (i<~10) vary and decrease slowly during the relaxation of the gas flow behind the shock wave. Indeed, the reason for slow variation is that VT transitions of molecules at first vibrational levels require a large gap of energy and monoquantum/multiquantum collisions are less effective in this condition. The concentrations of first vibrational levels decrease because molecules on these levels jump to higher levels due to VT transitions. This figure also shows that the VT model developed in this paper gives satisfactory results.

Figures 8, 9 and 10 present the vibrational temperature related to the first (i= 1), intermediate (i= 20) and last (i= 40) vibrational levels as a function of the distance behind the shock, calculated taking into account various VT energy exchanges. Monoquantum (s= 1) and multiquantum (s>1) transitions are considered. These figures show that all vibrational levels are influenced by multiquantum processes. However, relaxation of the first vibrational levels is finally achieved by VT collisional interaction between the 5 nearest levels. Densities of intermediate and higher levels depend, respectively, on 20 and almost all levels (~ 40) of the ground electronic state. The above behavior of all levels shows again the connection of the efficiency of multiquantum transitions with the magnitude of the energy jumps. Indeed, transitions from the first levels already occur for large energy jumps, so VT transitions are less efficient and only few nearest levels contribute to multiquantum mechanisms. However, energy levels are closer for higher quantum number of vibration, therefore vibrational distributions of higher levels are sensitive to the concentrations of more levels via VT collisions. The above results show that the number of multiquantum transitions needed in our simulations to capture state specific behavior increases with vibrational quantum number. This observation can be used to further improve the computational efficiency of our simulations by using different maximum allowable jumps depending on the vibrational quantum number of each state.

Figure 11 also shows the influence of VT processes on the evolution of the translational temperature with the distance behind the shock. We can see that this evolution is almost governed by first and intermediate vibrational levels. Indeed, the densities of higher levels are too weak compared to those of low levels, and thus cannot play a great role in the evolution of the macroscopic parameters of the gas flow with the initial conditions of this study.

Until now, only the ground electronic state of N_2 molecules was considered with its 49 total vibrational levels (i= 0,…,48). Now, the excited electronic states $A^3\Sigma$ and $B^3\Pi$ are implemented in the modeling and the figure 12 shows their evolution

with the distance behind the shock by considering various VT mechanisms and models. We can see that concentrations of excited electronic states still relax and do not reach the equilibrium state on a distance under of 10 cm. Moreover, their concentration is slightly higher in the case of monoquantum transitions because molecules reach excited electronic states via VE collisions (see Eq.(27)) from their first vibrational levels of the ground electronic state. Indeed, we saw above that populations of first levels related to the ground electronic state, are higher with monoquantum collisions (see figure 5).

However, as total mass fraction is equal to unity, we can see that densities of the excited electronic states remain very low under the free stream conditions of this study. Therefore, excited electronic states can be neglected in the actual modeling, and N_2 molecules on their ground electronic state give the main contribution to the predicted evolution of gas flow macroscopic parameters. Nevertheless, these excited electronic states must be taken into account if radiative intensities from the first positive N_2 system [58] are expected to be evaluated accurately. Note that Vibration-Electronic (VE) transitions observed for CO molecules [59,60] may effectively increase the concentration of excited electronic levels in the present modeling. Unfortunately, data of VE jumps related to N2 molecules are not available in our knowledge. The figure 12 also shows the good agreement of electronic levels concentration obtained using the present VT model with that of Nikitin et al. [46].

Further, it would be interesting to evaluate the increase in computing time required by the one-dimensional numerical code, when excited electronic states are considered along with supplemental vibrational levels. Indeed, the excited electronic states of N_2 molecules involves slightly more than double of the total number of vibrational levels (=106). The Table 1 shows that consideration of excited electronic states considerably increases the computing time with the VT model of Nikitin et al. [46]. Indeed, the latter model implies almost two days of computing time, whereas our model requires only about thirty minutes in the multiquantum case. While considering monoquantum transitions, the model developed in this study is also ~100 times faster.

IV. CONCLUSIONS

A new model is presented in this paper to calculate FHO rate coefficients related to VT transitions at high temperatures. This model is obtained with a quadrature method by using properties of Bessel's functions. Rates obtained with this model are in good agreement with those obtained with FHO models found in the literature. This model is used to simulate a pure N_2 gas flow behind a shock by considering a state-to-state approach. The macroscopic parameters behind the shock obtained using the proposed model are similar to those obtained on the basis of FHO models. The difference lies in the computing time where the model developed in this study is ~100 times faster. For the free stream conditions considered in this work we found a low concentration of N_2 molecules on their excited electronic states, therefore they can be neglected in the modeling. Nevertheless, their presence shows that additional vibrational levels increase strongly the computing time especially if multiquantum transitions are taken into account. Multiquantum processes are found to have a great influence on the evolution of macroscopic parameters of the N_2 gas flow behind the shock. Indeed, the relaxation of

high vibrational states is much faster than that of lower states, while a contrary behavior is observed if monoquantum transitions are considered. Moreover, with multiquantum processes, thermal equilibrium distribution of vibrational levels is attained at a considerably shorter distance behind the shock. Multiquantum jumps must be taken into account for all vibrational levels in modeling. However, the number of these transitions may decrease inversely as functions of the vibrational quantum numbers.

Further validation of the approximate model developed in this study can be performed using more accurate quantum calculations or experimental data on VT energy exchanges at high temperatures. However, this model can be efficiently utilized in nonequilibrium gas flow studies, because it can allow us consider excited electronic states of molecules and their multiquantum jumps on a very shorter computing time. We plan to extend the present work to investigate the effects of dissociation of N_2 molecules by accounting for VT multiquantum transitions obtained with the proposed model.

ACKNOWLEDGMENTS

P.V. and A.A. gratefully acknowledge the support of this project by the U.S. Air Force Research Laboratory (AFRL) and the DoD HPCMP's User Productivity Enhancement, Technology Transfer, and Training (PETTT) Program through High Performance Technologies, Inc. (HPTi). E.J. gratefully acknowledges financial support from the U.S. Air Force Office of Scientific Research (AFOSR).

REFERENCES

[1] M. Cacciatore, M. Capitelli, S. de Benedictis, M. Dilanardo and C. Gorse, in *Nonequilibrium Vibrational Kinetics*, edited by M. Capitelli, edited by M. Capitelli (Springer-Verlag, Berlin, 1986).

[2] C. S. Wang Chang and G. Uhlenbeck, University of Michigan, Research Report No.CM-681, 1951 (unpublished).

[3] S. Pascal and R. Brun, J. Phys. Rev. E **47**, 3251 (1993).

[4] E. V. Kustova and E. A. Nagnibeda, in *Rarefied Gas Dynamics 19*, (Oxford Science Publications, 1995) Vol. 1.

[5] E. V. Kustova and E. A. Nagnibeda, Chem. Phys. **208**, 313 (1996).

[6] G. Billing and E. Fisher , Chem. Phys. **43**, 395 (1979).

[7] G. Billing and R. Kolesnick , Chem. Phys. Lett. **200**, 382 (1992).

[8] G. Billing, in *Nonequilibrium Vibrational Kinetics*, edited by M. Capitelli (Springer-Verlag, Berlin, 1986) pp. 85-111.

[9] F. Esposito and M. Capitelli Chem. Phys. **418**, 581 (2006).

[10] F. Esposito, M. Capitelli and C.Gorse, Chem.Phys. 257, 193 (2000).

[11] F. Esposito and M. Capitelli, Chem. Phys. Lett, **302**, 49 (1999).

[12] E. Nagnibeda, in *Aerothermodynamics for Space vehicles*, edited by J. Hunt (ESA Publication Division, ESTEC, Noordwijk, Netherlands, 1995).

[13] F. Lordet, J. Meolans, A. Chauvin and R. Brun, Shock Waves **4**, 299 (1995).

[14] I. Adamovich, S. Macheret, J. Rich and C. Treanor, AIAA J. **33**, 1064 (1995).

[15] E. V. Kustova, A. Aliat and A. Chikhaoui, Chem.Phys. **344**, 638 (2001).

[16] A. Aliat, E. V. Kustova and A. Chikhaoui, Phys. Rev. E **68**, 056306 (2003).

[17] A. Aliat, E. V. Kustova and A. Chikhaoui, Chem. Phys. **314**, 37 (2005).

[18] S. Ruffin and C. Park, AIAA Pap. **92**, 0806 (1992).

[19] A. Chiroux de Gavelle de Roany, C. Flament, J. Rich, V. Subramanian and W. Warren, Jr., AIAA J. **31**, 119 (1993).

[20] B. Shizgal and F. Lordet, J. Chem. Phys. **104**, 3579 (1996).

[21] G. Colonna, M. Tuttafesta, M. Capitelli and D. Giordano, in *Rarefied Gas Dynamics 21* (CEPADUES, Toulouse, France, 1999) , Vol.2, pp.281-288.

[22] E. Josyula and W. F. Bailey, J. Thermophys. Heat Transfer **18**, 550 (2004).

[23] I. Armenise, M. Capitelli, G. Colonna and C. Gorse, J. Thermophys. Heat Transfer **10**, 397 (1996).

[24] M. Capitelli, I. Armenise and C. Gorse, J. Thermophys. Heat Transfer **11**, 570 (1997).

[25] E. Josyula, J. Thermophys. Heat Transfer **14**, 18 (2000).

[26] E. Josyula and W. F. Bailey, AIAA J. **41**, 1611 (2003).

[27] G. Candler, J. Olejniczak and B. Harrold, Phys.Fluids **9**, 2108 (1997).

[28] E. V. Kustova and E. Nagnibeda, Chem.Phys. **233**, 57 (1998).

[29] E.V. Kustova and A. Chikhaoui, Chem.Phys. **255**, 59 (2000).

[30] J. Arnold, V. Reis and H. Woodward, AIAA Pap.**65**, 0166 (1965).

[31] C. Park, in *Nonequilibrium Hypersonic Aerothermodynamics* (Wiley and Sons, New-York, 1990).

[32] G. Candler and C. Park, AIAA Pap. **88**, 2678 (1988).

[33] I. Adamovich, S. Macheret, J. Rich and C. Treanor, AIAA J. **33**, 1064 (1995).

[34] D. Secrest, B. Johnson and J. Chem.Phys. **45**, 4556 (1966).

[35] X. Chapuisat, G. Bergeron and J. M. Launay, Chem.Phys. **20**, 285 (1977).

[36] X. Chapuisat, G. Bergeron and J. M. Launay, Chem.Phys. **36**, 397 (1979).

[37] R. Schwartz, Z. Slawsky, K. Herzfeld, J. Chem. Phys. **20**, 1591 (1952).

[38] B. Gordiets, A. Osipov and L. Shelepin, in *Kinetic Processes in Gases and Molecular Lasers* (Gordon and Breach Science Publishers, Amsterdam, 1988).

[39] R. Bray, J. Phys. B. (Proc.Phys.Soc.) **1**, 705 (1968).

[40] E. Kerner, Can. J. Phys. **36**, 371 (1958).

[41] C. Treanor, J. Chem. Phys. **43**, 532 (1965).

[42] A. Zeleckow, D. Rapp, T. Sharp, J. Chem. Phys. **49**, 286 (1968).

[43] I. Adamovich, S. Macheret, J. Rich, C. Treanor, AIAA J. **33**, 1064 (1995).

[44] A. Aliat, Ph.D. thesis, (Universite de Provence, France, 2002).

[45] M. Lino da Silva, V. Guerra and J. Loureiro, J. Thermophys. Heat Transfer **21**, 40 (2007).

[46] E. Nikitin and A. Osipov, in *Kinetic and Catalysis* (VINITI, All-Union Institute of Scientific and Technical Information, Moscow, 1977), Vol.4, Chap.2 (in Russian).

[47] L. Landau and E. Teller, in *Theory of Sound Dispersion* (Physikalische Zeitschrift der Sowjetunion, 1936), Vol.10, p.34.

[48] K. Balla, O. S. Guk and M. Vicsek, Computing, **50**, 77 (1993).

[49] N. Dyson, in *Chromatographic Integration Methods*, (Royal Society of Chemistry, Cambridge, 1992).

[50] E. Nagnibeda, E. Kustova, in *Kinetic Theory of Transport and Relaxation processes in Nonequilibrium Reacting Gas Flows* (Saint Petersburg University, Saint Petersburg, 2003).

[51] A. Chikhaoui, J. Dudon, E. Kustova, E. Nagnibeda, Physica A **247**, 526 (1997).

[52] S. A. Losev and V. N. Yarygina, Russ.J.Phys.Chem.B **3**, 641 (2009).

[53] S. Edwards, J.Y. Roncin, F. Launay and F. Rostas, J. Mol. Spectrosc. **162**, 257 (1993).

[54] F. Roux and F. Michaud, Can. J. Phys. **68**, 1257 (1990).

[55] Y. Babou, P. Riviere, M.Y. Perrin and A. Soufiani, Int. J. Thermophys **30**, 416 (2009).

[56] E. Josyula, W. F. Bailey and C. J. Suchyta, AIAA Pap. **1579**, 1 (2009).

[57] C. W. Gear, in *Numerical Initial Value Problems in Ordinary Differential Equations* (Prentice-Hall, Englewood Cliffs, NJ, 1971).

[58] C. O. Laux and C. H. Kruger, J. Quant. Spectrosc. Radiat. Transfer **48**, 9 (1992).

[59] R.L. DeLeon and J.W. Rich, Chem. Phys. **107**, 283 (1986).

[60] E. Plönjes, P. Palm, J. W. Rich, I. V. Adamovich and W. Urban, Chem. Phys. **279**, 43 (2002).

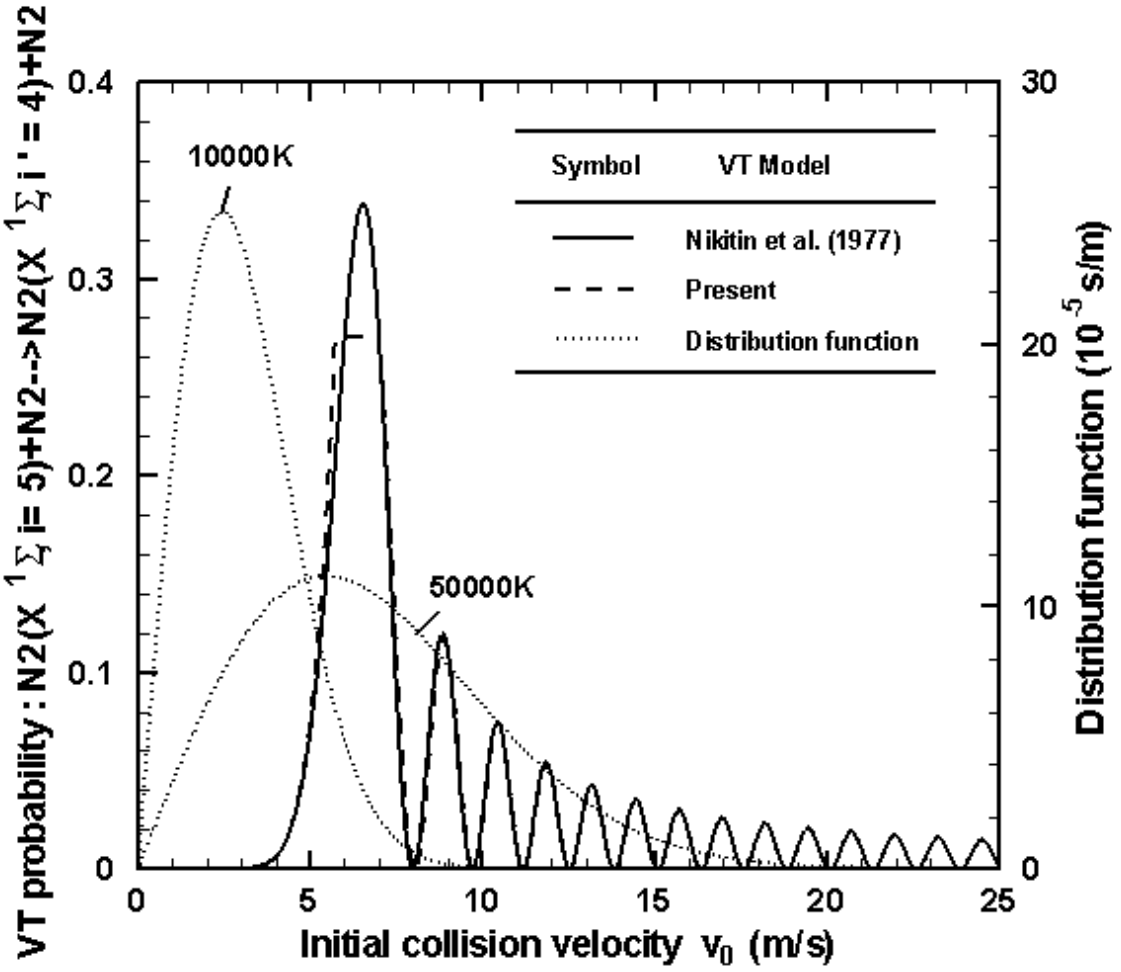

FIG.1. Monoquantum VT transition probability related to $N_2\left(X^1\Sigma, i=5\right)+N_2 \rightarrow N_2\left(X^1\Sigma, i'=4\right)+N_2$ process and the collisional distribution function (for 10000 and 50000K), both as functions of the initial relative velocity v_0. Various VT models are considered.

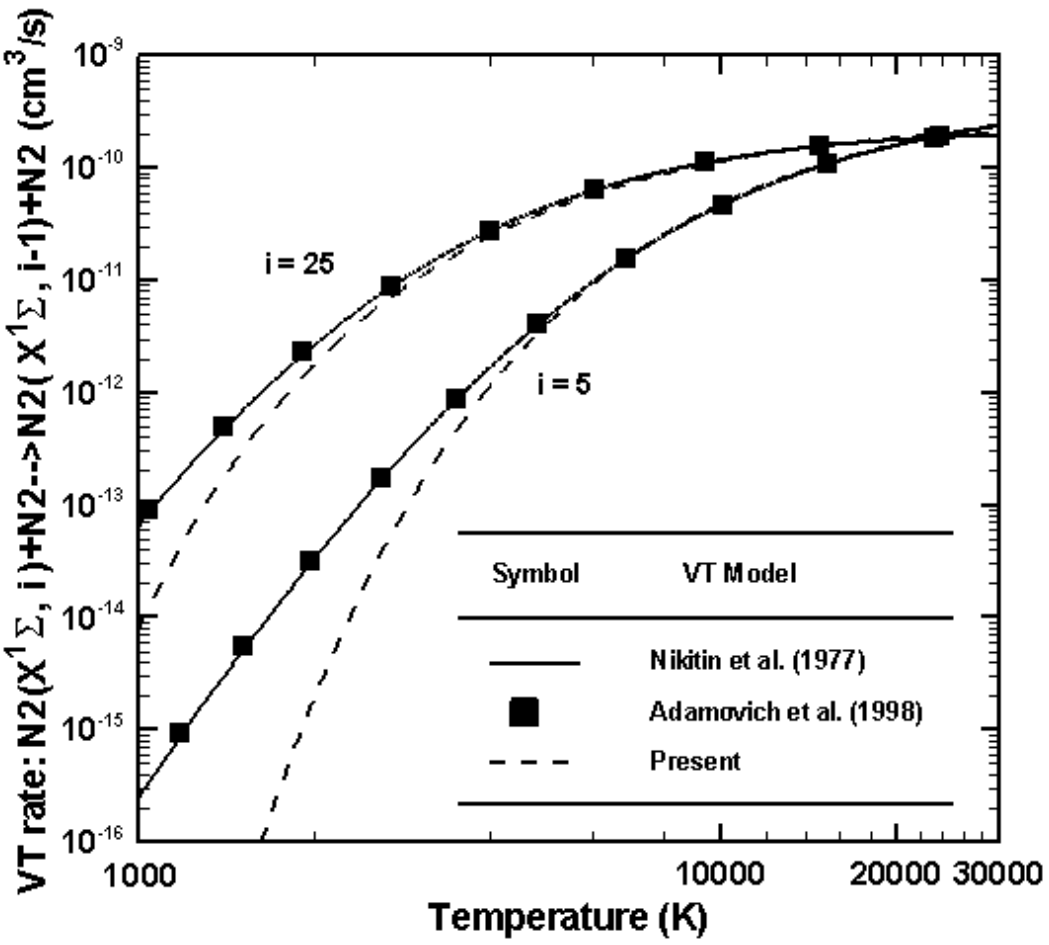

FIG.2. Monoquantum VT rate coefficients related to $N_2\left(X^1\Sigma, i=5,25\right)+N_2 \rightarrow N_2\left(X^1\Sigma, i-1\right)+N_2$ processes as functions of the translational temperature. Various VT models are considered.

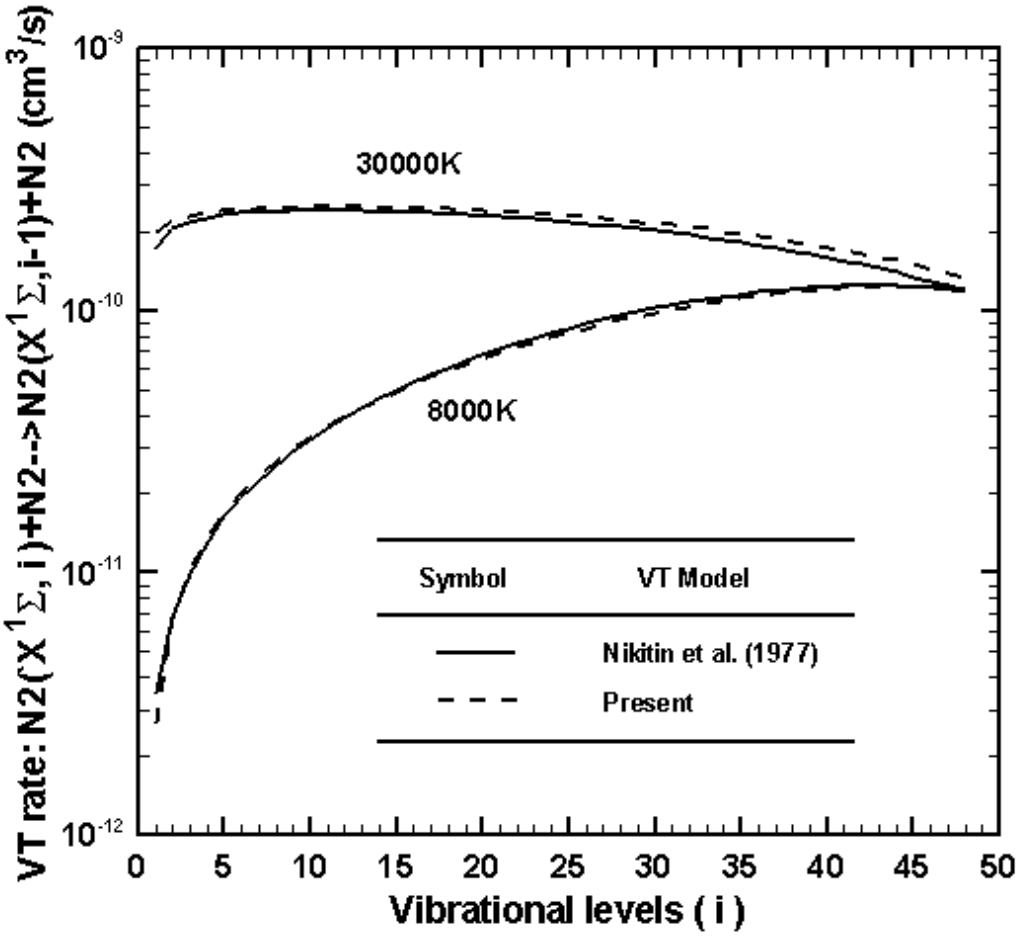

FIG.3. Monoquantum VT rate coefficients related to $N_2\left(X^1\Sigma, i\right)+N_2 \rightarrow N_2\left(X^1\Sigma, i-1\right)+N_2$ processes for various temperatures (8000 and 40000K) and as functions of the vibrational quantum numbers i. Various VT models are considered.

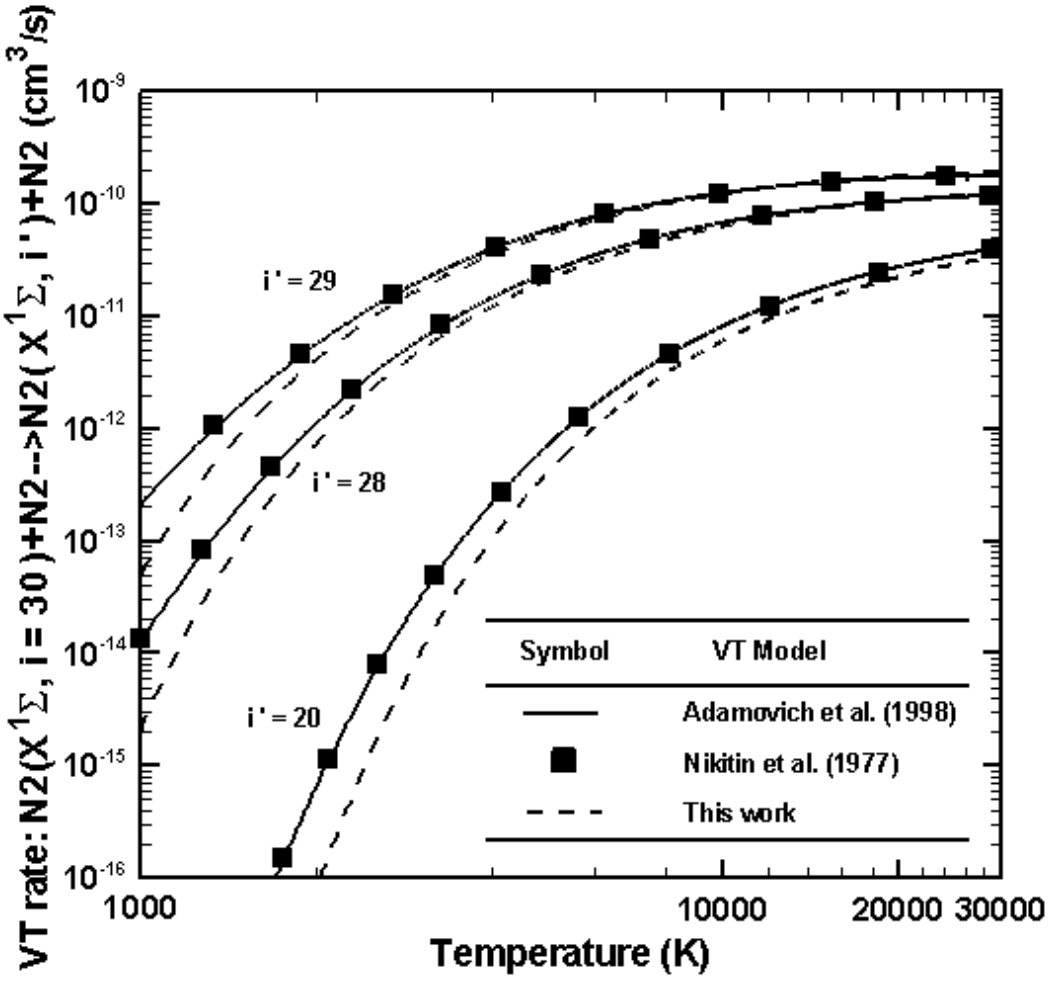

FIG.4. Multiquantum and monoquantum VT rate coefficients related to $N_2\left(X^1\Sigma, i=30\right)+N_2 \rightarrow N_2\left(X^1\Sigma, i'=20,28,29\right)+N_2$ processes and as functions of the translational temperature. Various VT models are considered.

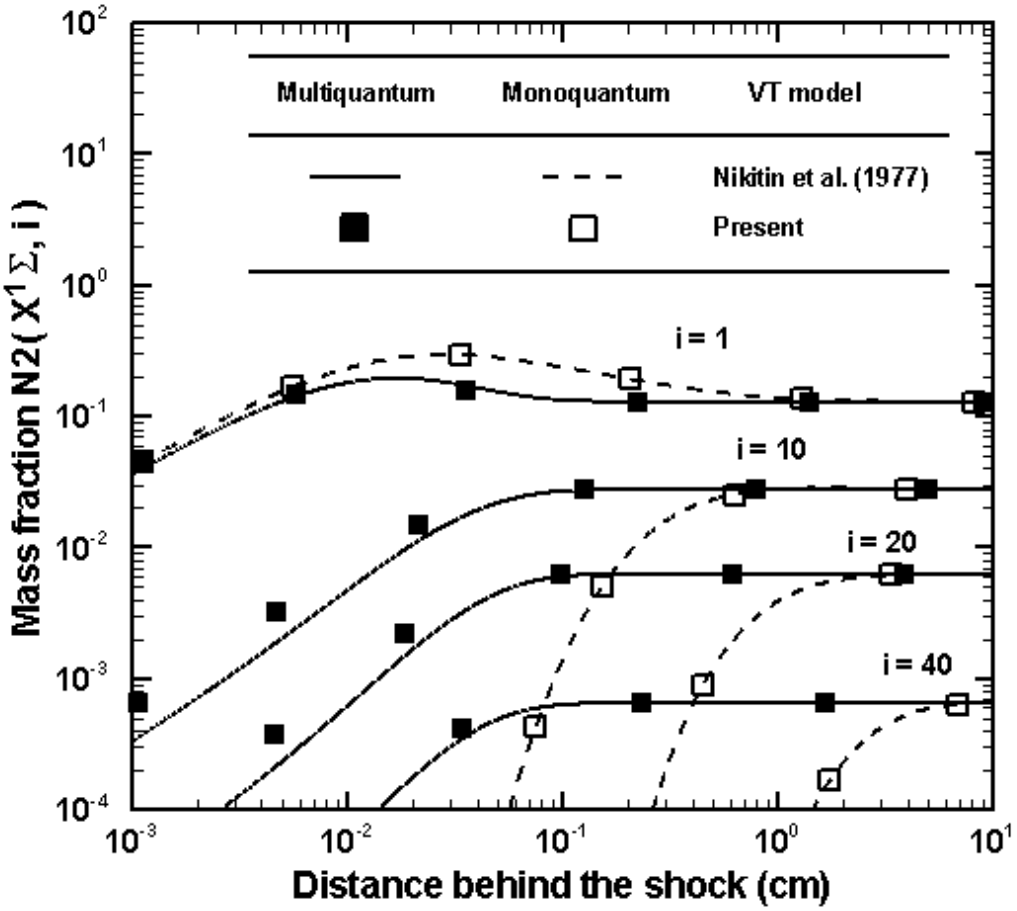

FIG.5. Vibrational distributions of $N_2\left(X^1\Sigma, i = 1,10,20,40\right)$ molecules as functions of the distance behind the shock. Multiquantum, monoquantum transitions and various VT models are considered. Free stream conditions: $P_\infty = 27Pa$, $T_\infty = 300K$ and $M_\infty = 19.82$.

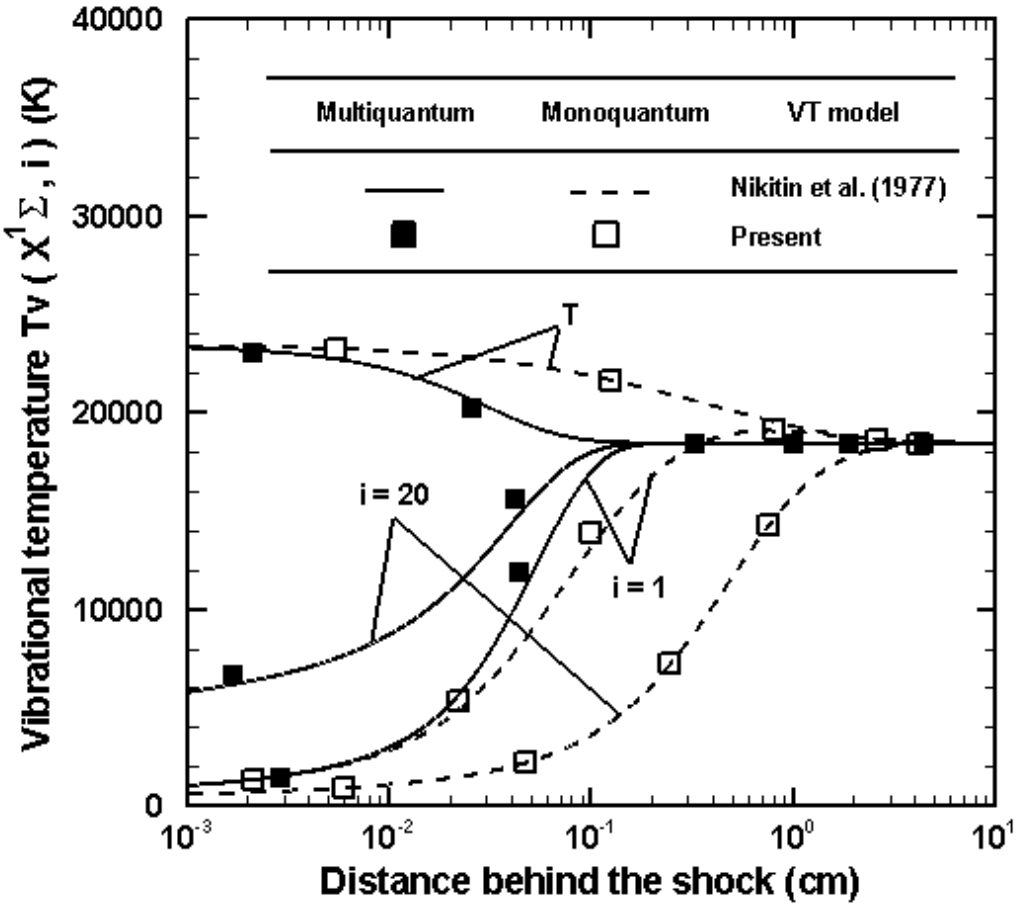

FIG.6. Evolution of local vibrational temperatures of $N_2\left(X^1\Sigma, i=1,\ 20\right)$ molecules and the translational temperature as functions of the distance behind the shock. Multiquantum, monoquantum transitions and various VT models are considered. Free stream conditions: $P_\infty = 27Pa$, $T_\infty = 300K$ and $M_\infty = 19.82$.

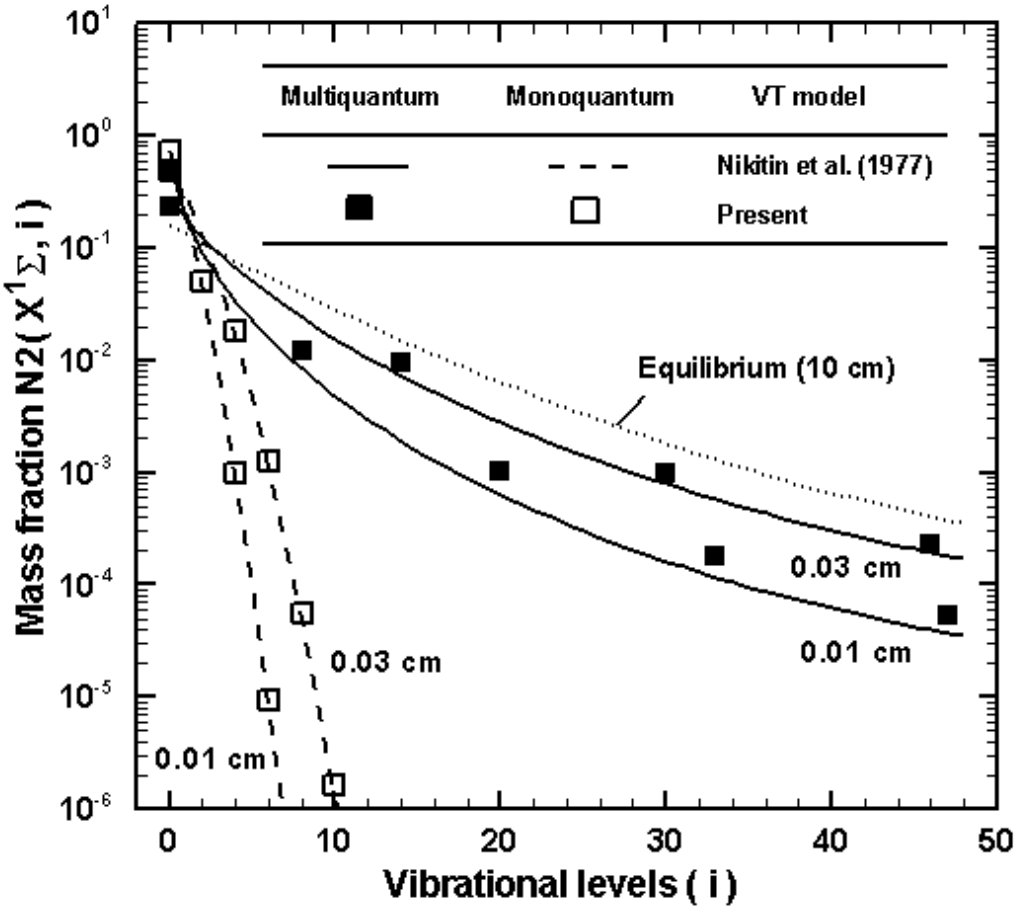

FIG.7. Vibrational distributions of molecules $N_2\left(X^1\Sigma, i\right)$ as functions of the vibrational quantum number i for various distances behind the shock. Multiquantum, monoquantum transitions and various VT models are considered. Free stream conditions: $P_\infty = 27Pa$, $T_\infty = 300K$ and $M_\infty = 19.82$.

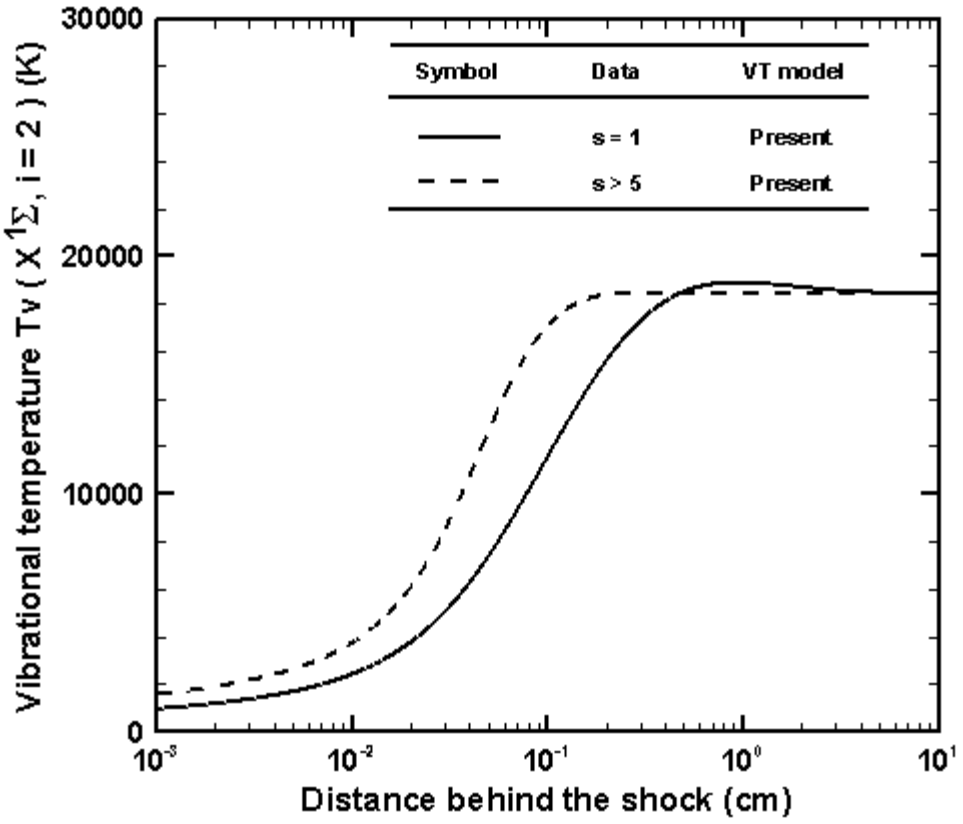

FIG.8. Evolution of the local vibrational temperature of $N_2\left(X^1\Sigma, i=1\right)$ molecules as functions of the distance behind the shock. Monoquantum (s=1) and multiquantum (s>1) transitions are considered. Free stream conditions: $P_\infty = 27Pa$, $T_\infty = 300K$ and $M_\infty = 19.82$.

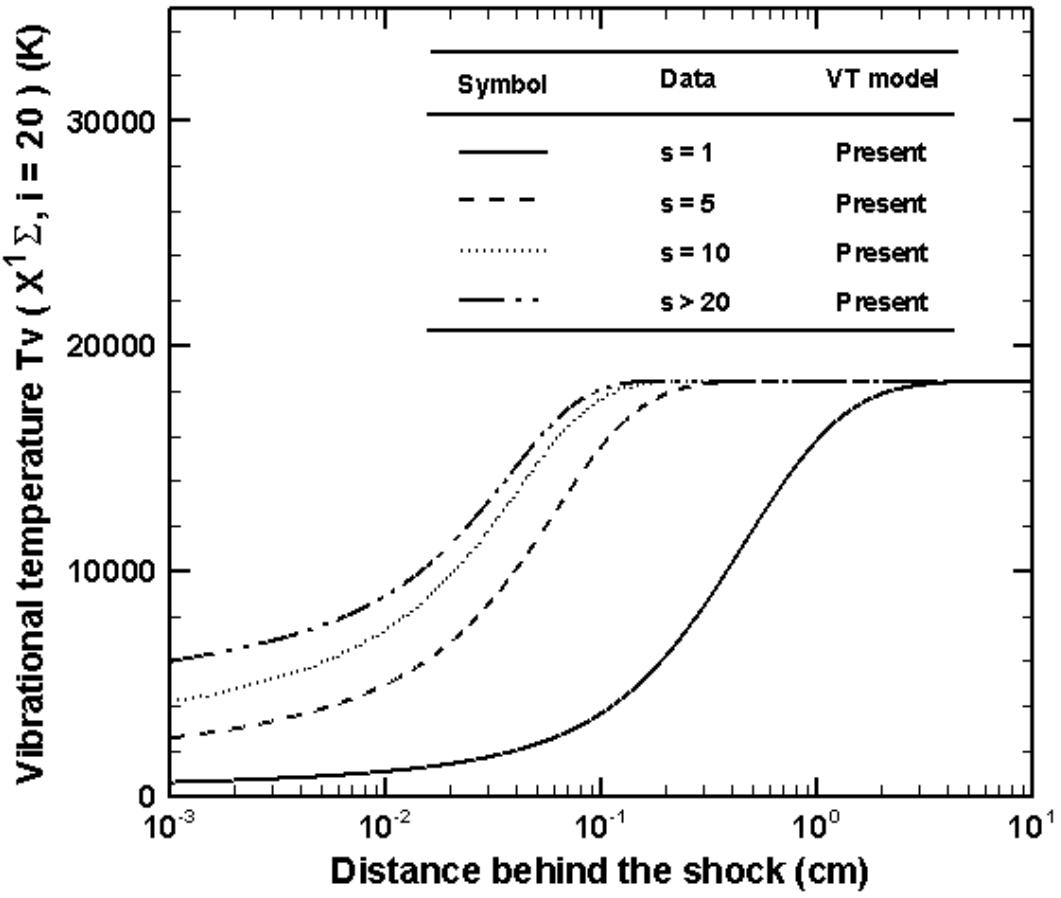

FIG.9. Evolution of the local vibrational temperature of $N_2\left(X^1\Sigma, i=20\right)$ molecules as functions of the distance behind the shock. Monoquantum (s=1) and multiquantum (s>1) transitions are considered. Free stream conditions: $P_\infty = 27Pa$, $T_\infty = 300K$ and $M_\infty = 19.82$.

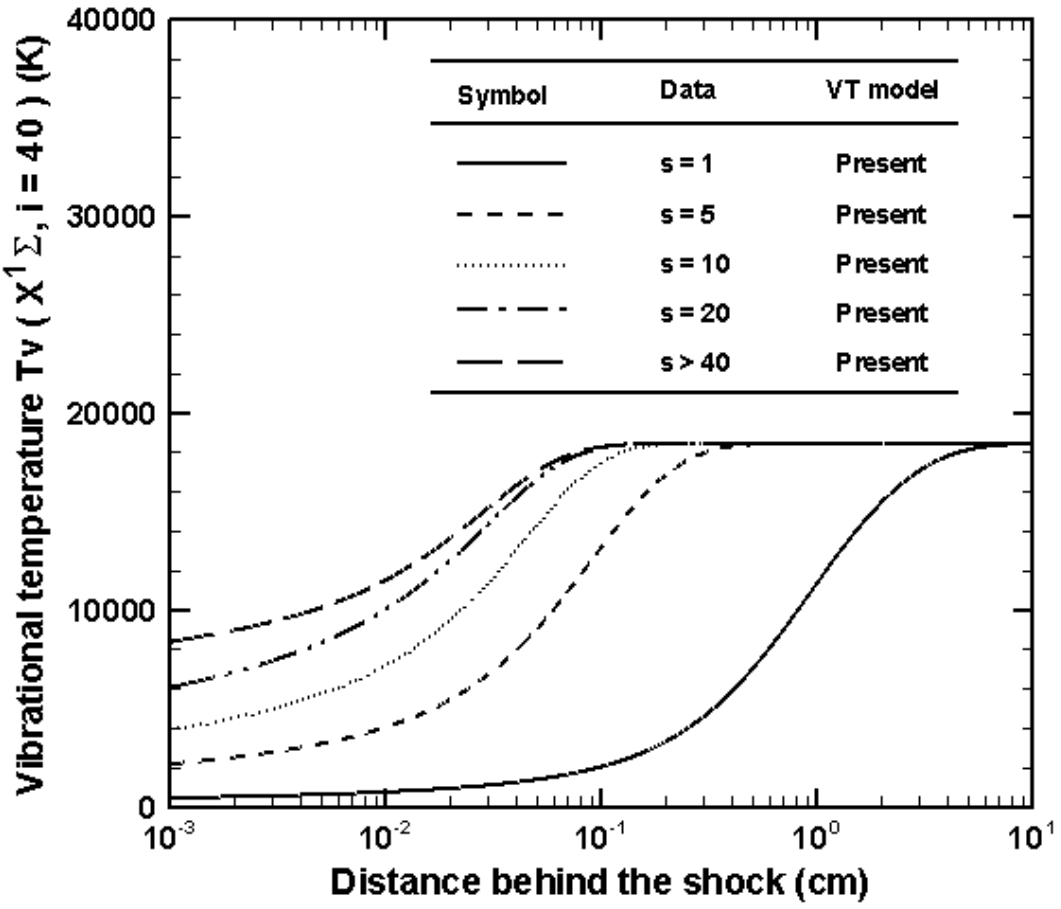

FIG.10. Evolution of the local vibrational temperature of $N_2\left(X^1\Sigma, i=40\right)$ molecules as functions of the distance behind the shock. Monoquantum (s=1) and multiquantum (s>1) transitions are considered. Free stream conditions: $P_\infty = 27Pa$, $T_\infty = 300K$ and $M_\infty = 19.82$.

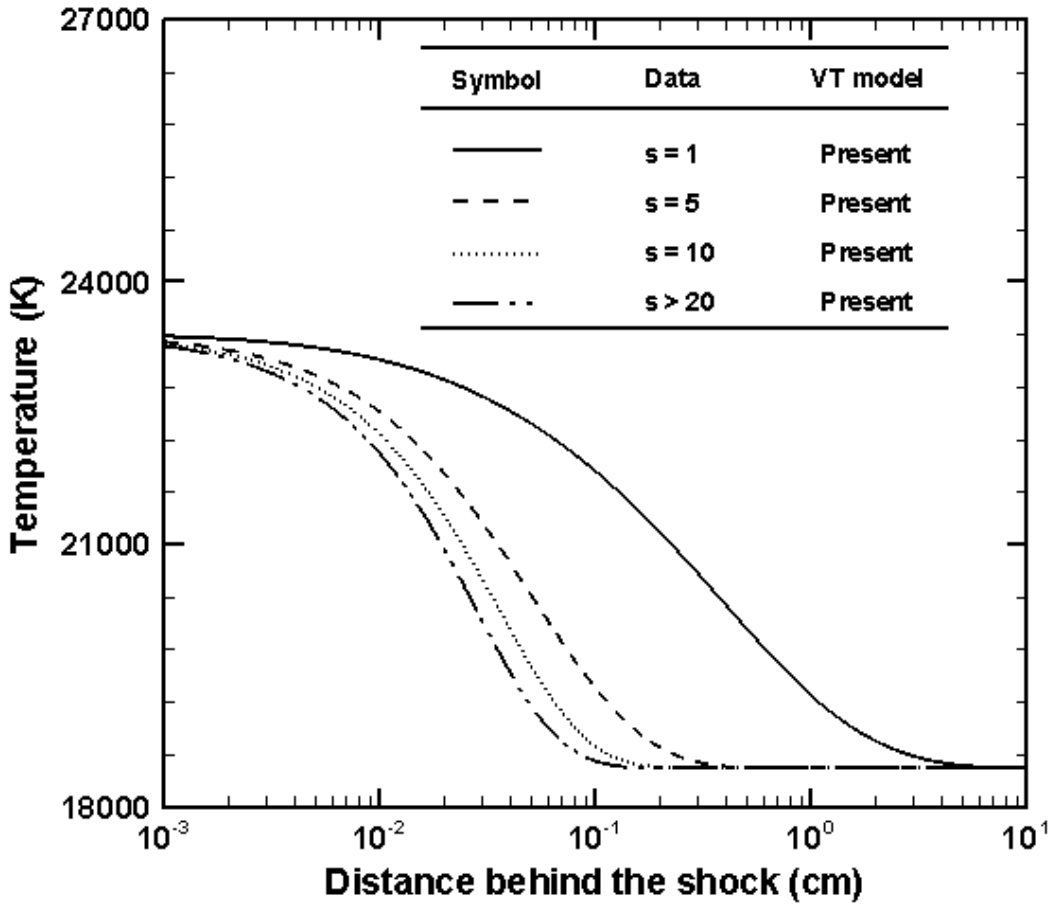

FIG.11. Evolution of the translational temperature as functions of the distance behind the shock. Monoquantum (s=1) and multiquantum (s>1) transitions are considered. Free stream conditions: $P_\infty = 27Pa$, $T_\infty = 300K$ and $M_\infty = 19.82$.

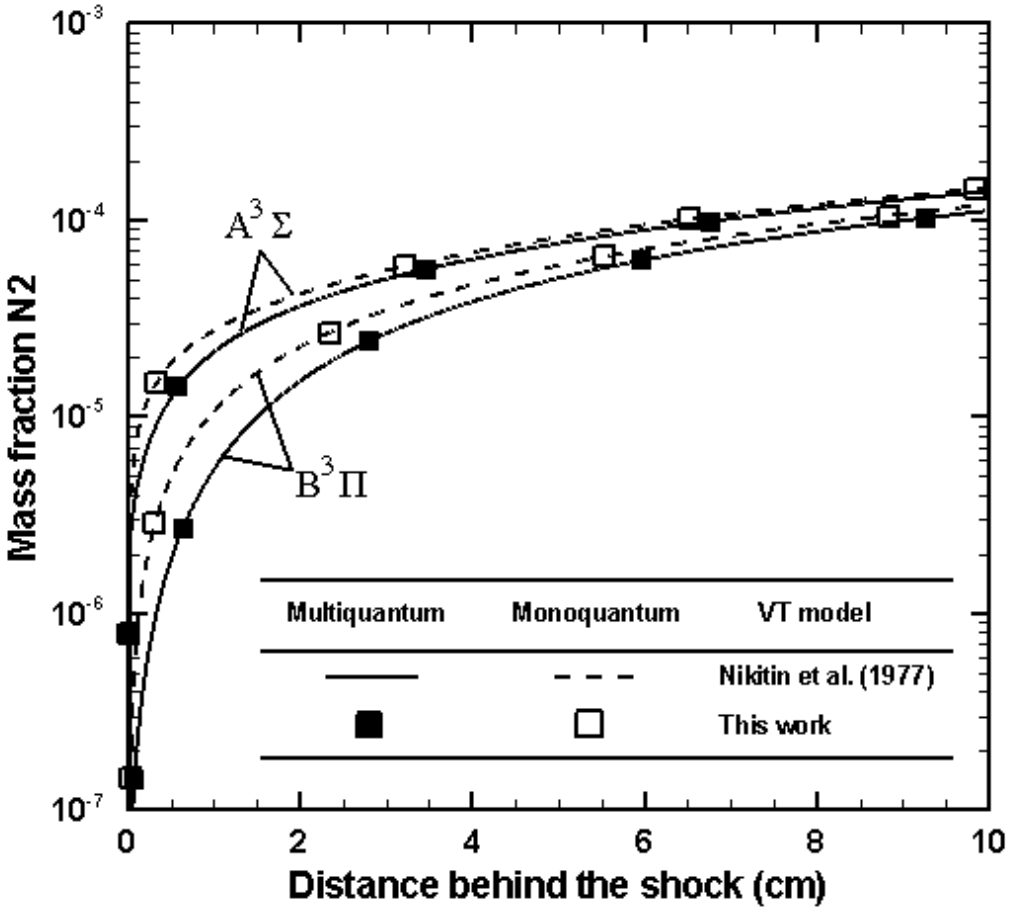

FIG.12. Evolution of concentrations of N_2 molecules on their excited states $A^3\Sigma$ and, $B^3\Pi$ as functions of the distance behind the shock. Multiquantum, monoquantum transitions and various VT models are considered. Free stream conditions: $P_\infty = 27Pa, T_\infty = 300K$ and $M_\infty = 19.82$.

Energy exchange + Electronic state	VT Model	Clock time
Multiquantum + Ground electronic state (49 levels)	Nikitin et al. [43] Present	5.9 hours 4.3 min
Monoquantum + Ground electronic state (49 levels)	Nikitin et al. [43] Present	25 min 14 s
Multiquantum + Ground and excited electronic states (109 levels)	Nikitin et al. [43] Present	1.8 days 31.2 min
Monoquantum + Ground and excited electronic states (109 levels)	Nikitin et al. [43] Present	3.7 hours 2 min

TABLE 1. Computing time estimated according to the various VT models, kind of vibrational energy exchanges (monoquantum and multiquantum) and the total number of vibrational levels in the modeling.

Appendix C: State-specific dissociation modeling with multiquantum Vibration-Translation transitions

A. Aliat[1*], P. Vedula[1*] and E. Josyula[2]

[1]School of Aerospace and Mechanical Engineering, University of Oklahoma, USA

[2]U.S. Air Force Research Laboratory, Wright-Patterson Air Force Base, Ohio 45433, USA

[*]Corresponding authors: azizaliat@ou.edu, pvedula@ou.edu

Abstract

An efficient state-specific model of dissociation using a quadrature approach is proposed by considering multiquantum Vibration-Translation (VT) transitions (between bound and quasibound vibrational levels) according to the Forced Harmonic Oscillator (FHO) theory. Application of this model to a pure N_2 gas flow behind a plane shock wave shows that dissociation has a large influence on intermediate and higher vibrational levels and is characterized by state-specific incubation distances, before which VT energy exchanges remain the dominant mechanism just behind the shock.

I. INTRODUCTION

The rate coefficients of Vibrational-Translational (VT) [1-5] and dissociation [5,6] obtained from accurate quasi-classical trajectories (QCT) calculations confirm that the assumption of a large difference among the characteristics times of relaxation of these processes is violated under high temperature conditions. This observation provides a convincing argument against using one-temperature or multi-temperature non-equilibrium flow descriptions based on some quasi-stationary distributions over internal energies. State-to-state (STS) models are thus developed and suggested [7] owing to their primary advantage of providing detailed descriptions of vibrational level populations, and thus avoiding the use of any unjustified assumptions of quasi-stationary distributions (e.g. Boltzmann, Treanor models or their modifications).

Recently, many studies have been carried out with STS approaches such as in high temperature N_2 and CO gas flows behind shock waves [8,9] and near blunt bodies [10,11]. It was shown that the updated VT model based on the forced harmonic oscillator (FHO) theory proposed by Adamovich et al. [12] satisfactorily describe the VT exchanges as the model takes into account multiquantum jumps which occur physically at high temperatures especially across close vibrational levels, i.e. at high quantum numbers. Nevertheless, calculations from the FHO analytical expressions are rather cumbersome and may easily reach the underflow/overflow limits of computing systems at high quantum numbers [13,14]. Very recently, an efficient VT model [15] was developed from the asymptotic approach of the Nikitin and Osipov [16] which gives the VT rates based on FHO theory in a large range of temperatures (<50,000K) and for all vibrational quantum numbers [9,12]. This model is based on a quadrature (integration)

method which considerably reduces the computing time, and thus can be used in CFD modeling by considering all multiquantum VT jumps. The modeling of vibrational energy exchanges is crucial [17] and must be done correctly because the dissociation is directly coupled to the vibration mode.

A variety of phenomenological and analytical dissociation models can be found into an exhaustive list in the reference [18]. One of the dissociation models of interest is based on the formalism of Macheret and Adamovich [19]. This formalism is based on the FHO theory but appears to have limitations for application in CFD modeling due to the consideration of a very high number of multiquantum VT transitions between bound and quasibound vibrational levels, which further results in a significant computational cost.

In this paper, we propose a state-specific dissociation model from the formalism of Macheret and Adamovich [19] by considering the fast VT model [15]. The state-specific rates of dissociation are compared to those found in the literature to evaluate the validity of the present model. The state-specific dissociation model is further implemented in a CFD code [15] to study the behavior of a shock heated N_2 gas flow via a state-to-state approach. The (monoquantum and multiquantum) VT transitions are considered and the influence of the vibration-dissociation coupling on the relaxation of the gas flow is investigated.

II. MODELING OF DISSOCIATION

The state-specific dissociation can be described by the following reaction:

$$A_i + M \rightarrow B + C + M\,, \tag{1}$$

where the diatomic molecule A dissociates from its vibrational state i to its two atomic components B and C; M is the collision partner. The related dissociation rate coefficient can be obtained from the following formalism of Macheret and Adamovich [19]:

$$k_i^{Diss}(T) = \sum_{\varepsilon_{i'} > D^e} k_{ii'}^{VT}(T), \tag{2}$$

where implicitly the total probability of collisional dissociation from the (bound) vibrational level i is equal to the sum over all final quasibound vibrational levels i' (of energy levels $\varepsilon_{i'}$) above the dissociation energy limit D^e. It is clear that the implementation of this formalism in CFD modeling is only possible if multiquantum VT rate coefficients are rapidly evaluated to avoid a large computing cost. For this purpose, we can use the fast VT model [15] obtained from the Nikitin and Osipov [16] approach which leads to k peaks over relative velocities of collision. Then, a quadrature (integration) method is applied to obtain the following VT rate coefficient [15]:

$$k_{ii'}^{VT}(T) \sim Z_M^{coll}(T)\left[\xi_{k=1} + \sum_{k>1} f_M^{distr}(v_{2,s,k}, T) h_{2,s,k}\, \Delta v_k\right] \tag{3}$$

where Z_M^{coll} and f_M^{distr} are the gas-kinetic frequency and the one-dimensional Maxwellian distribution function of speed related to the collisional partner M. Terms $v_{2,s,k}$, $h_{2,s,k}$ and Δv_k are the central positions, the height and the width at half-height of the kth peak. For k>1 the quadrature method is used by considering the triangle rule [20] and it is assumed

that the Maxwellian function is constant (evaluated on central velocities $v_{2,s,k}$) within the endpoints range of each peak (due to their narrowness). The integral $\xi_{k=1}$ is related to the first peak and was initially evaluated in a rough approximation to obtain VT rates at high temperatures (over ~ 4,000K). We also found that the analytical expression in Eq.(3) gives satisfactory VT rates at lower temperatures, when $\xi_{k=1}$ is evaluated by considering the mid-point quadrature method [21].

The energy of bound states are estimated with the usual Dunham expansion and the corresponding coefficients for N_2 molecules are given in the reference [22] to obtain $N_v^\alpha = 49\left(i = 0,...,N_v^\alpha - 1\right)$ total vibrational levels. However, the extrapolation of the Dunham expansion can not be used to estimate the energy of quasibound levels because it leads to a decrease of energy according to the vibrational quantum numbers [14] which is not realistic.

To overcome the limitation on the quasibound levels, we make the assumption that these levels are equivalent to free bound states and hence represent a region of continuum just over the energy of dissociation. This assumption implies that quasibound levels are very close to each other. It is well known that energy bound levels of anharmonic molecules become close to each other as functions of the vibrational quantum number. As a first approximation, we can use the energy gap between the last vibrational level and the dissociation limit as a reference to define the energy of quasibound levels. Further, we consider that the energy gap between quasibound levels is Δ times smaller of that of the above reference to increase the approach of each other, such as:

$$\varepsilon_{i'} = D_e + i'\left(D_e - \varepsilon_{i=N_v^\alpha - 1}\right)/\,\Delta \qquad \left(i' \geq 1\right), \tag{4}$$

where (unlike the Dunham expansion) we can see that this relation allows having energy levels which always increase as functions of the vibrational quantum number i'.

The dissociation rate coefficients of $N_2\left(i = 0,10,30\right) + N \rightarrow 3N$ processes are illustrated in figure1. The rates from the expression Eq.(2) are compared to those accurate of Bourdon et al.[23] obtained from QCT calculations of Esposito et al. [6] $\left(\leq 10{,}000K\right)$ and from the NASA Ames database [24,25] $\left(> 10{,}000K\right)$. We can see that rates of the dissociation model in Eq.(2) are in satisfactory agreement with data of Bourdon et al. [23] by considering $\Delta = 10^3$ in Eq.(4). This observation shows that the present assumption of free quasibound levels is a good approximation and the parameter $\Delta = 10^3$ (that we adopt thereafter) implies that these levels are enough close to each other to represent the continuum.

III. APPLICATION AND DISCUSSION

We apply the governing Euler equations [8,9] to study a one-dimensional, inviscid, pure N_2 gas flow behind a plane shock wave by a state-to-state approach. The free stream conditions are those of Josyula et al. [10], i.e. a Mach of 19.83, a temperature of 300K and a pressure of 27Pa. The kinetic scheme of this gas flow consists of VT transitions:

$$N_2(i) + M \leftrightarrow N_2(i') + M \tag{5}$$

and the dissociation reaction :

$$N_2(i) + M \rightarrow 2N + M, \tag{6}$$

where collisional partners M are molecules and atoms of nitrogen on their ground electronic states $X^1\Sigma$ and ^4S, respectively. Monoquantum and all multiquantum VT jumps are considered in Eq. (5). Note that in this study, Vibration-Vibration (VV) transitions [8,12] and the recombination reaction [26] are not considered because they play a minor role at high temperatures.

The vibrational distributions of N_2 molecules for various distances behind the shock are shown in figure 2. In order to isolate the pure dissociation effect, we present results for cases with and without dissociation while considering multiquantum VT transitions. For both of these cases, we can see that the behavior close to the shock (distance of $10^{-3} cm$) is similar which implies that the effect of multiquantum VT transitions is dominant compared to that of dissociation. However, the effect of dissociation first becomes effective for higher vibrational levels (distance of 10^{-2}cm) due the high state-specific rates on high levels (see the figure 1). Dissociation is thus preferential and implies a finite state-specific incubation distance (when the dissociation becomes effective) for each vibrational level. Owing to the presence of these state-specific incubation distances of dissociation, the vibrational-dissociation coupling does not allow the distributions to reach the thermal equilibrium in small distances, as in $\sim 0.1 cm$ behind the shock when only multiquantum VT transitions alone are considered. Figure 2 also shows that the dissociation mechanism results in a great decrease in the population of intermediate and higher vibrational levels (as in distances 1 and 10 cm). Note that the population of lowest levels decreases especially from VT transitions to populate the upper levels.

The state-specific local vibrational temperature is defined as follows:

$$T_v(i) = \frac{\left(\varepsilon_i - \varepsilon_{i=0}\right)}{k_b \ln\left(N_i / N_{i=0}\right)}, \tag{7}$$

which is obtained by assuming a Boltzmann distribution over vibrational energies. Terms k_b and N_i are the constant of Boltzmann and the number density of the vibrational level i. The evolution of the translational temperature T, vibrational temperatures of first $(i = 5)$, intermediate $(i = 30)$ and higher $(i = 45)$ levels are shown in the figure 3.

This figure confirms the dominant influence of multiquantum VT jumps just behind the shock as all state-specific vibrational temperatures are found to increase (with both vibrational quantum number and distance from the shock) in this region. This observation can be attributed to the fact that multiquantum VT transitions are more efficient for higher levels which are close to each other for anharmonic molecules. However, these state-specific vibrational temperatures are found to have an extremum whose location corresponds to state-specific incubation distances of the dissociation. These distances are related to each level and decrease with increase in vibrational energy levels. The rapid

decrease of the vibrational temperature T_v $(i=45)$ compared to those of intermediate $(i=30)$ and lower $(i=5)$ levels is the consequence of the preferential nature of the dissociation. Figure 3 also shows that the lowest levels quickly reach the thermochemical equilibrium at $\sim 2.10^{-1} cm$ because we saw above that their populations are especially governed by the VT transitions. This is not the case for intermediate and higher levels because of the vibration-dissociation coupling causing the translational temperature T to decrease even at distances over $10cm$. This decrease is more rapid in the presence of multiquantum transitions, in comparison to the monoquantum case, because intermediate and higher vibrational levels are more effectively populated [15], and thus more molecules tend to dissociate due to the preferential dissociation (which is endothermic in nature).

The chemical concentrations as functions of distances behind the shock are illustrated in the figure 4 by considering the dissociation of molecules and the various (monoquantum and multiquantum) VT energy exchanges. The degree of dissociation is found lower with consideration of pure monoquantum transitions as they greatly underestimate greatly the populations of intermediate and higher levels [15] and the dissociation is preferential. However, the discrepancy on the atomic production is not so high between the two kinds of VT jumps (i.e. monoquantum and multiquantum), as this production comes essentially from low vibrational levels which are the most populated.

IV. CONCLUSIONS

In this paper a state-specific model of dissociation is proposed from the formalism of Macheret and Adamovich [19]. Our model considers multiquantum VT transitions between bound and quasibound vibrational levels and is based on the Forced Harmonic Oscillator (FHO) theory. The present state-specific model is developed using a quadrature method in order to reduce computing cost and to facilitate its efficient implementation in computational fluid dynamics (CFD) modeling. The quasibound levels are assumed to be equivalent to free bound states and represent the continuum of states with energy above the dissociation limit. State-specific rate coefficients obtained in this study are in good agreement with those found in the literature. The dissociation model is implemented to investigate the behavior of a pure N_2 gas flow behind a plane shock wave by a state-to-state approach. The dissociation reaction has a great influence on intermediate and high levels because of its preferential character. However, up to a certain (state-specific) incubation distance for each vibrational level behind the shock, the populations of levels are primarily governed by VT energy exchanges. These incubation distances are found to decrease as functions of vibrational quantum numbers as the dissociation is preferential. Consideration of monoquantum VT jumps alone is found to result in a lower degree of dissociation compared to that of multiquantum VT transitions.

ACKNOWLEDGMENTS

P.V. and A.A. gratefully acknowledge the support of this project by the U.S. Air Force Research Laboratory (AFRL) and the DoD HPCMP's User Productivity Enhancement, Technology Transfer, and Training (PETTT) Program through High Performance Technologies, Inc. (HPTi). E.J. gratefully acknowledges financial support from the U.S. Air Force Office of Scientific Research (AFOSR).

REFERENCES

[1] G. Billing and E. Fisher , Chem. Phys. **43**, 395 (1979).

[2] G. Billing and R. Kolesnick , Chem. Phys. Lett. **200**, 382 (1992).

[3] G. Billing, in *Nonequilibrium Vibrational Kinetics*, edited by M. Capitelli (Springer-Verlag, Berlin, 1986) pp. 85-111.

[4] F. Esposito and M. Capitelli Chem. Phys. **418**, 581 (2006).

[5] F. Esposito, M. Capitelli and C.Gorse, Chem.Phys. **257**, 193 (2000).

[6] F. Esposito, I. Armenise and M. Capitelli, Chem. Phys., **331**, 1 (2006).

[7] E. Nagnibeda, E. Kustova, in *Kinetic Theory of Transport and Relaxation processes in Nonequilibrium Reacting Gas Flows* (Saint Petersburg University, Saint Petersburg, 2003).

[8] A. Aliat, E. V. Kustova and A. Chikhaoui, Phys. Rev. E **68**, 056306 (2003).

[9] A. Aliat, E. V. Kustova and A. Chikhaoui, Chem. Phys. **314**, 37 (2005).

[10] E. Josyula, W. F. Bailey and C. J. Suchyta, J. Thermophys. Heat Transfer **25**, 1 (2011).

[11] E. Josyula and W. F. Bailey, AIAA J. **41**, 1611 (2003).

[12] I. Adamovich, S. Macheret, J. Rich and C. Treanor, AIAA J. **33**, 1064 (1995).

[13] A. Aliat, Ph.D. thesis, (Universite de Provence, France, 2002).

[14] M. Lino da Silva, V. Guerra and J. Loureiro, J. Thermophys. Heat Transfer **21**, 40 (2007).

[15] Aliat, P. Vedula, E. Josyula, Phys. Rev. E, (2010) (in press).

[16] E. Nikitin and A. Osipov, in *Kinetic and Catalysis* (VINITI, All-Union Institute of Scientific and Technical Information, Moscow, 1977), Vol.4, Chap.2 (in russian).

[17] J. W. Rich and C. E. Treanor, Ann. Rev. Fluid Mech. **2** (1970) 355.

[18] Physical and Chemical Processes in Gas Dynamics: Cross Sections and Rate Constants for Physical and Chemical Processes. Volume I. Vol.196 of Progress in Astronautics and Aeronautics, 2002.

[19] S. Macheret and I. Adamovich, J. Chem. Phys. **113**, 7351 (2000).

[20] N. Dyson, in *Chromatographic Integration Methods*, (Royal Society of Chemistry, Cambridge, 1992).

[21] http://en.wikipedia.org/wiki/Numerical_integration

[22] S. Edwards, J. Y. Roncin, F. Launay, F. Rostas, J. Mol. Spectrosc. **162**, 257 (1993).

[23] A. Bourdon, M. Panesi, A. Brandis, T. E. Mangin, G. Chaban, W. Huo, R. Jaffe and D.W. Schwenke, in Proceedings of the 2008 Summer Program (Center for Turbulence Research, Stanford University, Stanford, 2008).

[24] R. Jaffe , D. Schwenke, G. Chaban, and W. Huo, AIAA 2008-1208, 46th AIAA Aerospace Science Meeting and Exhibit, Reno, NV, Jan 7-10.

[25] D. Schwenke, G. Chaban, R. Jaffe and W. Huo, AIAA 2008-1209, 46th AIAA Aerospace Science Meeting and Exhibit, Reno, NV, Jan 7-10.

[26] Y. Stupochenko, S. Losev and A. Osipov, in *Relaxation in Shock Waves*, (Springer-Verlag, Berlin, Heidelberg, New-York, 1967).

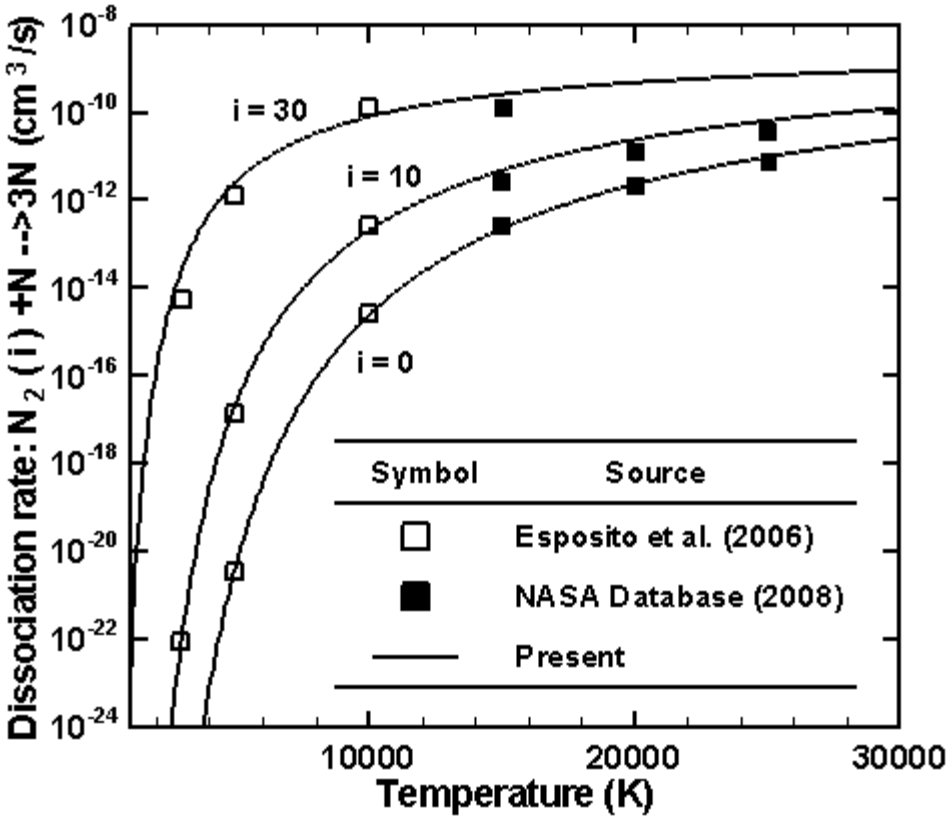

FIG.1. State-specific dissociation rate coefficients of $N_2(i = 0,10,30) + N \rightarrow 3N$ as functions of the translational temperature. Various dissociation models are considered.

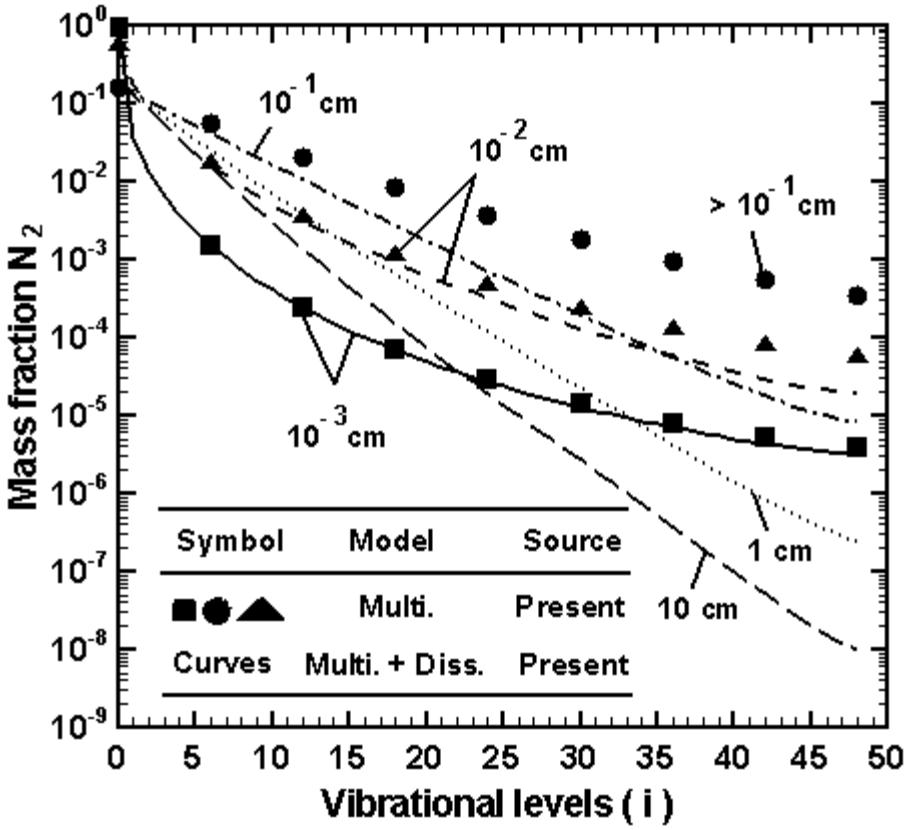

FIG.2. Vibrational distributions of N_2 molecules as functions of vibrational quantum numbers i. Various distances behind the shock and physicochemical processes (dissociation and multiquantum VT transitions) are considered.

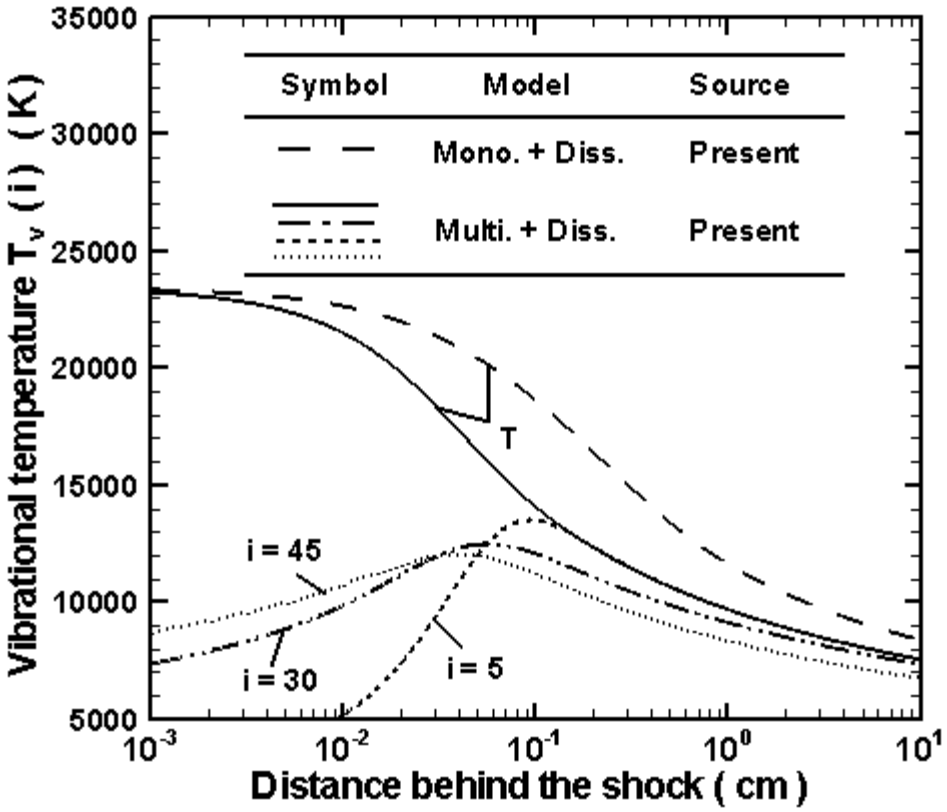

FIG.3. Evolutions of the translational T and local vibrational temperatures T_v of $N_2(i = 5,30,45)$ molecules as functions of the distance behind the shock. Dissociation and (monoquantum and multiquantum) VT processes are considered.

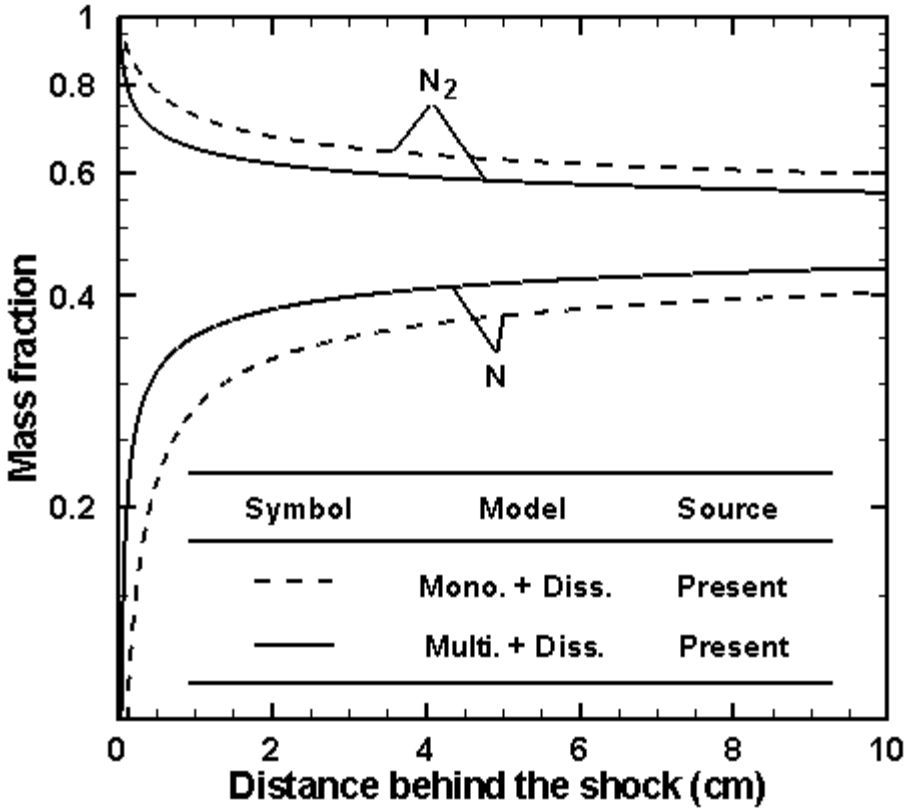

FIG.4. Mixture composition as functions of the distance behind the shock. Various physicochemical models (dissociation, monoquantum and multiquantum VT transitions) are considered.

Appendix D: State-specific modeling of radiation in reactive nonequilibrium gas flows

A. Aliat[1*], P. Vedula[1*] and E. Josyula[2]

[1]School of Aerospace and Mechanical Engineering, University of Oklahoma, Norman, Oklahoma 73019, USA

[2]U.S. Air Force Research Laboratory, Wright-Patterson Air Force Base, Dayton, Ohio 45433, USA

[*]Corresponding authors: azizaliat@ou.edu, pvedula@ou.edu

Abstract

A radiation model is developed to obtain the evolution of band intensities according to the state-to-state (STS) approach. Implementation of this model to investigate the behavior of a nonequilibrium reactive and radiative N_2 gas flow behind a plane shock wave, shows that the radiation intensity remains weak and the gas flow is far from radiative equilibrium. Similar intensities are predicted by both STS and commonly used local thermodynamic equilibrium (LTE) approaches. However, the coupling (between the physico-chemical and radiative processes) increases with the radiation intensity.

I. INTRODUCTION

Although equations of aerothermochemistry that account for radiative effects have been considered by many authors [1-3], they are usually based on the local thermodynamic equilibrium (LTE) assumption and are often considered independently from the collision processes. This uncoupled description can imply noticeable errors in estimated values of radiation intensities and radiative heat flux in strongly nonequilibrium high temperature reacting gas flows. To overcome this limitation, a state-to-state (STS) model was proposed in [4] on the basis of a rigorous kinetic theory with coupled vibrational relaxation, chemical reactions and radiative transitions. The advantage of the STS approach is the lack of the assumption of quasi-stationary distributions over internal energies which is often used in the literature (multi-temperature models) and is invalid for high temperature conditions [5]. The equations of conservation of state-specific population, momentum and energy developed in [4] contain radiative terms which allow for accounting of strong coupling between the physicochemical and radiative mechanisms. These radiative terms are governed by the microscopic radiative transfer equation that describes the evolution of specific intensity (i.e. the distribution function of photons) which is a spectral quantity. It is extremely challenging (from a numerical standpoint) to directly obtain this photonic distribution over the entire range of frequencies.

In this paper, we extend the theoretical study [4] by proposing a detailed model for radiation using a STS approach. In our model, the photonic distribution is obtained via the band intensities which are governed by a radiative transfer equation using a macroscopic approach. This model is implemented to generalize previous studies [5,6] and investigate the effects of radiation in a N_2 gas flow behind a plane shock wave, with the consideration of the dissociation of molecules, multiquantum Vibration-Translation (VT) and Vibration-Electronic (VE) transitions. The radiation from our STS approach is compared to that obtained from commonly used (i) LTE assumption and (ii) the uncoupled form (where hydrodynamic and radiative conservation equations are independently treated). The influence of the radiation on the gas relaxation behind the shock is also investigated.

II. STATE-SPECIFIC RADIATIVE MODEL

For a 1D stationary gas flow behind a normal shock, the microscopic radiative transfer equation reads [4]:

$$\frac{dI_\nu}{dx} = \sum_{\alpha,i,j,p,\alpha',i',j',p'} h\nu_{\alpha ijp,\alpha'i'j'p'}\,\phi_\nu\left(\nu-\nu_{\alpha ijp,\alpha'i'j'p'}\right) \times\left[A_{\alpha ijp,\alpha'i'j'p'}N_{\alpha ijp}+\left(B_{\alpha ijp,\alpha'i'j'p'}N_{\alpha ijp}-B_{\alpha'i'j'p',\alpha ijp}N_{\alpha'i'j'p'}\right)I_\nu\right] , \quad (1)$$

where the variable x corresponds to the direction of the shock wave propagation. Terms h and I_ν correspond to Planck's constant and specific intensity (based on frequency ν), respectively. The number density $N_{\alpha i j p}$ is related to the quantum level of the electronic α, vibration i, rotational j and the parity p states. The primed (unprimed) letters in the above equation refer to the lower (upper) quantum level. Terms $B_{\alpha'i'j'p',\alpha i j p}$,

$B_{\alpha i\,j\,p,\alpha' i' j' p'}$ and $A_{\alpha i\,j\,p,\alpha' i' j' p'}$ are the Einstein coefficients of induced absorption, induced and spontaneous emissions, respectively, which are related through the detailed balance principle, as $A_{\alpha ijp,\alpha' i' j' p'} / B_{\alpha ijp,\alpha' i' j' p'} = 2h\nu^3_{\alpha ijp,\alpha' i' j' p'} / c^2$ and $s_{\alpha ijp} B_{\alpha i\,j\,p,\alpha' i' j' p'} = s_{\alpha' i' j' p'} B_{\alpha' i' j' p',\alpha i\,p}$, where c is the speed of light. The term $s_{\alpha i\,j\,p}$ corresponds to the product of statistical weights related to rotational $(=2j+1)$, vibrational (=1 for diatomic molecules) and electronic s_α $\left(=(2-\delta_{0,\Lambda})\times(2S+1)\right)$ states. The factor $(2S+1)$ corresponds to the spin multiplicity, while $(2-\delta_{0,\Lambda})$ is the degeneracy due to the Λ-doubling. The Kronecker delta $\delta_{0,\Lambda}$ has a non-zero value equal to 1 only if $\Lambda = 0$, where Λ is the absolute value of the projected total electronic angular momentum on the internuclear axis which is equal to 0, 1, 2,…for $\Sigma, \Pi, \Delta, \ldots$ molecular states, respectively.

The Einstein coefficient related to the spontaneous emission $\alpha, i, j, p \rightarrow \alpha', i', j', p'$ can be separated into two parts:

$$A_{\alpha i\,j\,p,\alpha' i' j' p'} = A_{\alpha i,\alpha' i'} \frac{S_{jp,j'p'}}{2j+1}, \qquad (2)$$

where $A_{\alpha i,\alpha' i'}$ is the Einstein coefficient for spontaneous emission related to the band transition $\alpha, i \rightarrow \alpha', i'$. The Hönl-London factors (or rotational line strengths) $S_{j\,p,j'p'}$ are related to branches $j\,p \rightarrow j'\,p'$ and are normalized to obey the sum rule [7] as $\sum_{j'p'} S_{j\,p,j'p'} = (2-\delta_{0,\Lambda}\delta_{0,\Lambda'})(2S+1)(2j+1)$. The term ϕ_ν in Eq.(1) corresponds to the spectral line profile, which is assumed to be the same for the three kinds of radiative mechanisms (e.g. spontaneous emission, induced emission/absorption). This profile satisfies the normalization condition, i.e. $\int_0^\infty \phi_\nu(\nu - \nu_{\alpha i\,j\,p,\alpha' i' j' p'})\,d\nu = 1$, where $\nu_{\alpha i\,j\,p,\alpha' i' j' p'}$ is the central frequency of radiative transitions $\alpha, i, j, p \leftrightarrow \alpha', i', j', p'$.

In this study the radiative lines are assumed to follow the Doppler broadening (at low pressures and high temperatures) and do not overlap in the spectrum. Hence, from Eqs. (1) and (2) with the above properties on Einstein coefficients, Hönl-London factors and the broadening profile, integrating over frequency and summing over the rotational levels (which follow a Boltzmann distribution with translational temperature T), the microscopic radiative transfer equation Eq.(1) can be expressed (at the macroscopic scale) as,

$$\frac{dI_{\alpha i,\alpha' i'}}{dx} = h\nu_{\alpha i,\alpha' i'} B_{\alpha i,\alpha' i'} N_{\alpha i} \left[\frac{2h\nu^3_{\alpha i,\alpha' i'}}{c^2} + \sqrt{\frac{\ln(2)}{2\pi}} \frac{I_{\alpha i,\alpha' i'}}{\gamma^D_{\alpha i,\alpha' i'}} \left(1 - \frac{s_\alpha}{s_{\alpha'}} \frac{N_{\alpha' i'}}{N_{\alpha i}}\right) \right], \qquad (3)$$

which governs the evolution of the band intensity $I_{\alpha i,\alpha' i'}$ (power per area and per solid angle) behind the shock. The above equation is also obtained by assuming that the various branches emit on their mean central frequency which is the frequency of the corresponding band $\nu_{\alpha i,\alpha' i'}$ $\left(=\tilde{\nu}_{\alpha i\,j\,p,\alpha' i' j' p'}\right)$. The term $\gamma^D_{\alpha i,\alpha' i'}$ $\left(=\nu_{\alpha i,\alpha' i'}\sqrt{2k_b T/mc^2}\right)$ corresponds to the full width at half maximum of the Doppler line profile, which is also

expressed according to the translational temperature T, the mass of the molecule m and the constant of Boltzmann k_b. Note that the number density $N_{\alpha i}$ in Eq. (3) is related to the electro-vibrational level (α, i).

We can compare our STS radiation model in Eq. (3) with those based on the local thermodynamic equilibrium (LTE) assumption often used in the literature. In the LTE assumption, a Boltzmann distribution over vibrational energy at a vibrational (translational) temperature T_v (T) is considered. This vibrational temperature is defined by the ratio of the two first vibrational levels in the ground electronic state, as these levels are the most populated and thus characterizes the thermodynamic evolution of the gas flow [8]. Then, from the Eq. (3) we have the following LTE radiative transfer equation:

$$\frac{dI_{\alpha i,\alpha'i'}}{dx} = h\nu_{\alpha i,\alpha'i'} B_{\alpha i,\alpha'i'} \frac{N_\alpha}{Q_\alpha^{vib}(T_v)} \exp\left(-\frac{\varepsilon_i^\alpha}{k_b T_v}\right) \times \left\{ \frac{2h\nu_{\alpha i,\alpha'i'}^3}{c^2} + \sqrt{\frac{\ln(2)}{2\pi}} \frac{I_{\alpha i,\alpha'i'}}{\gamma_{\alpha i,\alpha'i'}^D} \left\{ 1 - \frac{s_\alpha}{s_{\alpha'}} \frac{N_{\alpha'}}{N_\alpha} \frac{Q_\alpha^{vib}(T_v)}{Q_{\alpha'}^{vib}(T_v)} \exp\left[-\frac{\left(\varepsilon_{i'}^{\alpha'} - \varepsilon_i^\alpha\right)}{k_b T_v} \right] \right\} \right\} \quad , \tag{4}$$

where $Q_\alpha^{vib}(T_v)$ and $N_\alpha \left(= \sum_i N_{\alpha i}\right)$ are the partition function of vibration (related to the electronic state α) at the vibrational temperature T_v and the number density of molecules on the electronic state α, respectively. The term ε_i^α corresponds to the energy of the vibrational level i of the corresponding electronic state α.

The nonequilibrium gas flow can be considered as a black body if it reaches the thermal (at the rotational-translational temperature T) and the radiative $\left(dI_{\alpha i,\alpha'i'}/dx = 0\right)$ equilibria. From this consideration, we can derive an expression for the black body band intensity from Eq. (3), as

$$I_{\alpha i,\alpha'i'}^{eq} = \frac{2h\nu_{\alpha i,\alpha'i'}^3}{c^2} \gamma_{\alpha i,\alpha'i'}^D \sqrt{\frac{2\pi}{\ln(2)}} \left[\frac{Q_\alpha^{vib}(T)}{Q_{\alpha'}^{vib}(T)} \exp\left(\frac{h\nu_{\alpha i,\alpha'i'}}{k_b T}\right) - 1 \right]^{-1} . \tag{5}$$

Radiative terms present in STS equations of conservation [4] can be expressed from the band intensities $I_{\alpha i,\alpha'i'}$ obtained from the Eq. (3). The radiative source term present in the state-specific conservation equation of continuity is given by:

$$\begin{aligned} R_{c\alpha i}^{rad} = & \sum_{\alpha''} \sum_{i''} \sum_{j,p,j'',p''} \int_0^\infty \int_{4\pi} \phi_\nu\left(\nu - \nu_{\alpha''i''j''p'',\alpha i j p}\right) \left[A_{\alpha''i''j''p'',\alpha i j p} N_{\alpha''i''j''p''} \right. \\ & \left. + \left(B_{\alpha''i''j''p'',\alpha i j p} N_{\alpha''i''j''p''} - B_{\alpha i j p,\alpha''i''j''p''} N_{\alpha i j p} \right) I_\nu \right] d\nu \, d\boldsymbol{\Omega}_\nu \\ & - \sum_{\alpha'} \sum_{i'} \sum_{j,p,j',p'} \int_0^\infty \int_{4\pi} \phi_\nu\left(\nu - \nu_{\alpha i j p,\alpha'i'j'p'}\right) \left[A_{\alpha i j p,\alpha'i'j'p'} N_{\alpha i j p} \right. \\ & \left. + \left(B_{\alpha i j p,\alpha'i'j'p'} N_{\alpha i j p} - B_{\alpha'i'j'p',\alpha i j p} N_{\alpha'i'j'p'} \right) I_\nu \right] d\nu \, d\boldsymbol{\Omega}_\nu \quad , \end{aligned} \tag{6}$$

where α" (α') correspond to the upper (lower) electronic level compared to that α. The term $d\mathbf{\Omega}_\nu$ corresponds to the solid angle related to the direction of propagation of the photon with a frequency ν. Using a similar approach as that used to derive the macroscopic radiative transfer equation Eq. (3), Eq. (6) can be expressed as:

$$R_{c\alpha i}^{rad} \approx \frac{4\pi}{h}\left(\sum_{\alpha"} \sum_{i"} \frac{1}{\nu_{\alpha"i"j",\alpha i\, j}} \frac{dI_{\alpha"i",\alpha i}}{dx} - \sum_{\alpha'} \sum_{i'} \frac{1}{\nu_{\alpha i\, j,\alpha'i'j'}} \frac{dI_{\alpha i,\alpha'i'}}{dx} \right) \quad , \quad (7)$$

where the radiation field is assumed to be isotropic in this study. Similarly, the derivative of the radiative heat flux in the total energy conservation equation [4] can be expressed as:

$$\begin{aligned} \frac{dq_{rad}}{dx} &= \int_0^\infty \int_{4\pi} \frac{dI_\nu}{dx} \mathbf{\Omega}_\nu . \mathbf{n}\, d\nu\, d\mathbf{\Omega}_\nu \\ &= 2\int_0^\infty \frac{dI_\nu}{dx} d\nu \int_0^{\pi/2} \cos\varphi \sin\varphi\, d\varphi \int_0^{2\pi} d\vartheta \approx 2\pi \sum_{\alpha,i,\alpha',i'} \frac{dI_{\alpha i,\alpha'i'}}{dx} , \end{aligned} \quad (8)$$

where $\mathbf{n}$ and $\mathbf{\Omega}_\nu$ correspond to unit vectors along the direction of propagation of the shock and the photon ν, respectively. Terms φ $\left(\mathbf{\Omega}_\nu . \mathbf{n} = \cos\varphi\right)$ and θ are the zenith and azimuth angles in spherical coordinates, respectively.

III. RESULTS AND DISCUSSION

The present radiation model is implemented to generalize previous studies [5,6] for a pure N_2 gas flow behind a plane shock wave (1D steady Euler equations). The nitrogen molecules are considered to be in their ground $\left(X^1\Sigma\right)$ and excited ($A^3\Sigma$ and $B^3\Pi$) electronic states, while undergoing the dissociation, Vibration-Translation (VT) and Vibration-Electronic (VE) energy exchanges. We use the VT and the dissociation models developed in [5,6] which are based on the forced harmonic oscillator (FHO) theory that accurately accounts for multiquantum jumps at high temperatures. These multiquantum jumps play a significant role in the evolution of intermediate and higher vibrational levels [5,6] which can have strong line strengths, and thus can have a major part on the amount of emitted radiation. The first positive system of N_2 molecules is considered in this study and is described by the following spontaneous emissions:

$$N_2\left(B^3\Pi, i\right) \rightarrow N_2\left(A^3\Sigma, i\right) + h\nu, \quad (9)$$

and induced emissions/absorptions,

$$N_2\left(B^3\Pi, i\right) + h\nu \leftrightarrow N_2\left(A^3\Sigma, i\right) + 2h\nu . \quad (10)$$

A summary of spectroscopic data for the various electronic states of N_2 molecules can be found in [9], while the Einstein coefficients related to band transitions are given in [10]. The free stream conditions are those of Josyula et al. [11], i.e. a Mach number of 19.83, a temperature of 300K and a pressure of 27Pa. A higher Mach number (= 25) is also considered to make comparisons and study its influence on the numerical results.

The influence of the radiation on the molecular concentrations is shown in figure 1. It is clear that radiative mechanisms play a significant role on the concentration of $N_2\left(B^3\Pi\right)$ molecules, as they correspond to upper levels of the first positive radiative system. Their concentration is found to be lower when the radiation is taken into account, due to radiative de-excitations to the lower electronic state $A^3\Sigma$. However, the number of these de-excitations is small compared to the population of $N_2\left(A^3\Sigma\right)$ molecules which remains nearly unchanged. With a higher Mach number, the population of N_2 molecules (in their ground electronic state $X^1\Sigma$) decreases especially from their intermediate and higher vibrational levels due the preferential character of the dissociation [6]. As the VE energy exchanges are connected to the population of these vibrational levels, the production of electronically excited molecules is thus decreased.

The intensity of radiation emitted by the gas flow remains low as shown in figure 2. This observation comes from weak excitation of N_2 molecules in the $B^3\Pi$ electronic state (see figure 1). The radiation intensity is thus mainly governed by spontaneous emissions (induced emissions/absorptions mechanisms play a minor part) which cause a constant decrease of the $N_2\left(B^3\Pi\right)$ population observed in figure 1. Figure 2 also shows that the gas flow can not be considered as a black body, as the radiation intensity is ~6 orders of magnitude lower than that in a radiative equilibrium condition. The radiation is found lower with increasing Mach number since the emissive $N_2\left(B^3\Pi\right)$ molecules are less formed from VE transitions as explained in the preceding paragraph.

The importance of coupling between the physicochemical and the radiative processes is observed in figure 3. The case without coupling tends to overestimate the emitted radiation and the discrepancy increases with its intensity. However, the radiation models based on LTE assumptions (at the vibrational temperature T_v and the rotational-translational temperature T) lead to similar intensities as that obtained with the STS approach. Small discrepancies observed between the STS and LTE approaches could come from of the weak intensity of radiation emitted by the gas flow. With a higher Mach, we have similar observations but with a weaker radiation due to the lower concentration of $N_2\left(B^3\Pi\right)$ molecules (see figure 1).

The radiation (from STS and LTE approaches) has a minor influence on the rotational-translational temperature, as shown in figure 4. The evolution of the macroscopic gas parameters are essentially governed by the behavior of most populated species (i.e. on their ground electronic states) which do not contribute to the emitted radiation from the first positive radiative system. The evolution of the vibrational temperature shows that the LTE assumption based radiation models according to different temperatures (T_v and T) become similar in a $\sim 1mm$ distance behind the shock. At a higher Mach, this distance is shorter $\left(\sim 0.5mm\right)$.

IV. CONCLUSION

A detailed state to state (STS) model for radiation is proposed by considering the spectroscopic properties (including fine structure, Einstein coefficients, Doppler broadening, Λ-doubling, the sum rule of Hönl-London factors) and is applied in CFD

modeling. This model is based on the radiative transfer equation to obtain the macroscopic band intensities (which are used to evaluate radiative terms in the hydrodynamic conservation equations in order to account for strong coupling between the physicochemical and radiative mechanisms). Both STS and local thermodynamic equilibrium (LTE) approaches are implemented to study the behavior of a radiative and reactive N_2 gas flow behind a plane shock. The first positive system of N_2 molecules is considered, i.e. radiative transitions between the excited electronic states $B^3\Pi$ and $A^3\Sigma$ (including spontaneous emissions and induced emissions/absorptions). Owing to the effects of radiation, the concentration of $N_2\left(B^3\Pi\right)$ molecules decreases due to radiative de-excitations. The dominant contribution to radiation arises from spontaneous emissions (compared to induced mechanisms) because the radiation intensity remains weak in this study. The flow is far from radiative equilibrium and therefore can not be treated as a black body. The influence of the coupling between the physicochemical and radiative processes increases according to the radiation intensity. Note that the commonly used LTE assumption gives predictions that are similar to that obtained from the STS approach. This observation can be attributed to weak radiation intensity obtained in this study. Radiation is found to decrease with increase in Mach number, as the preferential dissociation is more efficient which further lowers the production of electronically excited molecules from Vibrational-Electronic (VE) transitions. The radiative mechanisms have a minor influence on the evolution of macroscopic gas parameters such as the rotational-translational temperature, as they are primarily governed by the species in their ground electronic states.

ACKNOWLEDGMENTS

P.V. and A.A. gratefully acknowledge the support of this project by the U.S. Air Force Research Laboratory (AFRL) and the DoD HPCMP's User Productivity Enhancement, Technology Transfer, and Training (PETTT) Program through High Performance Technologies, Inc. (HPTi). E.J. gratefully acknowledges financial support from the U.S. Air Force Office of Scientific Research (AFOSR).

REFERENCES

[1] G. Candler, and C. Park, in *AIAA Thermophysics, Plasmadynamics and Lasers Conference* (American Institute of Aeronautics and Astronautics, San Antonio, TX, 1988), AIAA 88-2678.

[2] C. Park, in *Nonequilibrium Hypersonic Aerothermodynamics* (Wiley and Sons, New York, 1990).

[3] J. Arnold, V. Reis, and H. Woodward, AIAA J. **3**, 2019 (1965).

[4] E. Kustova, and A. Chikhaoui, Chem. Phys. **255**, 59 (2000).

[5] A. Aliat, P. Vedula, and E. Josyula, Phys. Rev. E, **83**, 026308 (2011).

[6] A. Aliat, P. Vedula, and E. Josyula, Phys. Rev. E, **83**, 037301 (2011).

[7] E. Whiting, A. Schadee, J. Tatum, J. Hougen, and R.W. Nicholls, J. Mol. Spectrosc. **80**, 249 (1980).

[8] T. Magin, M. Panesi, A. Bourdon, R. Jaffe, and D. Schwenke *Internal energy excitation and dissociation of molecular nitrogen in a compressible flow* (Center for Turbulence Research, Stanford University, Annual Research Briefs, 2009).

[9] Y. Babou, Ph. Riviere, M. -Y. Perrin, and A. Soufiani, Int. J. Thermophys. **30**, 416 (2009).

[10] C. Laux, and C. Kruger, J. Quant. Spectrosc. Radiat. Transfer **48**, 9 (1992).

[11] E. Josyula, W. F. Bailey, and C. J. Suchyta, in *47th AIAA Aerospace Sciences Meeting including the New Horizons Forum and Aerospace Exposition* (American Institute of Aeronautics and Astronautics, Orlando, FL, 2009), AIAA 2009-1579.

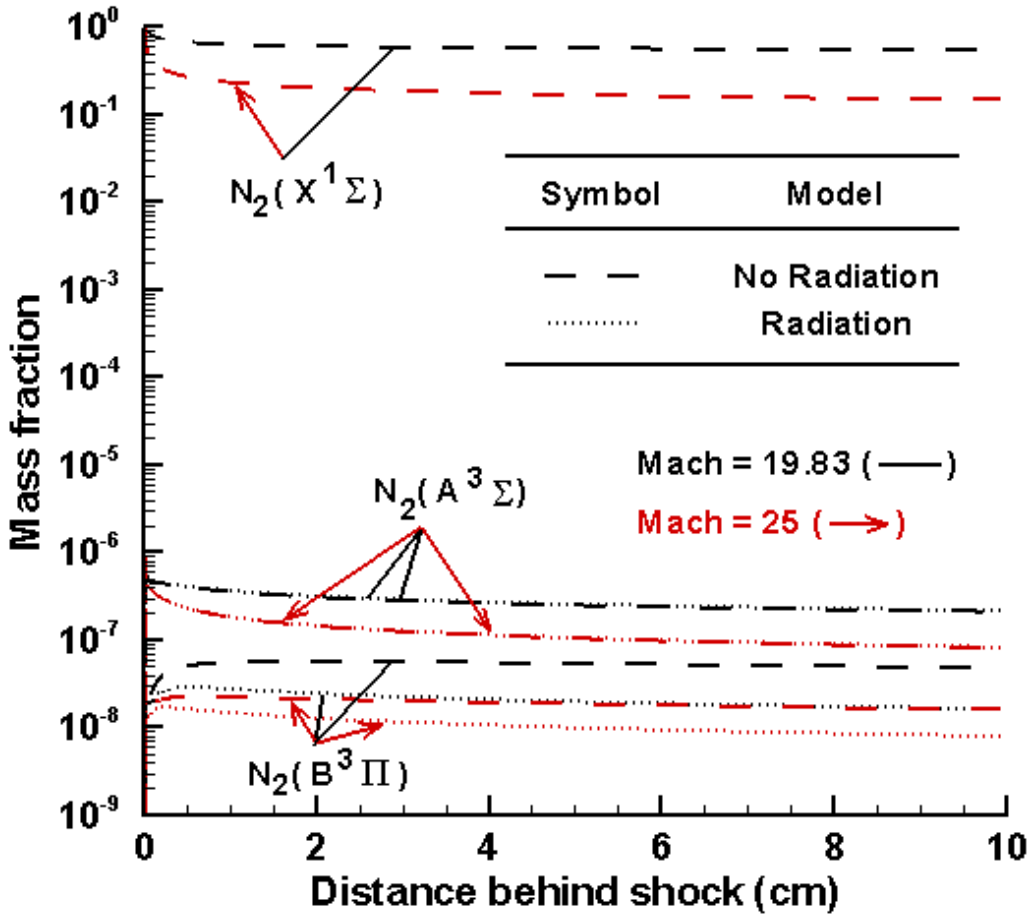

Fig. 1. Concentrations of N_2 molecules behind the shock with/without the effects of the radiation at different Mach numbers.

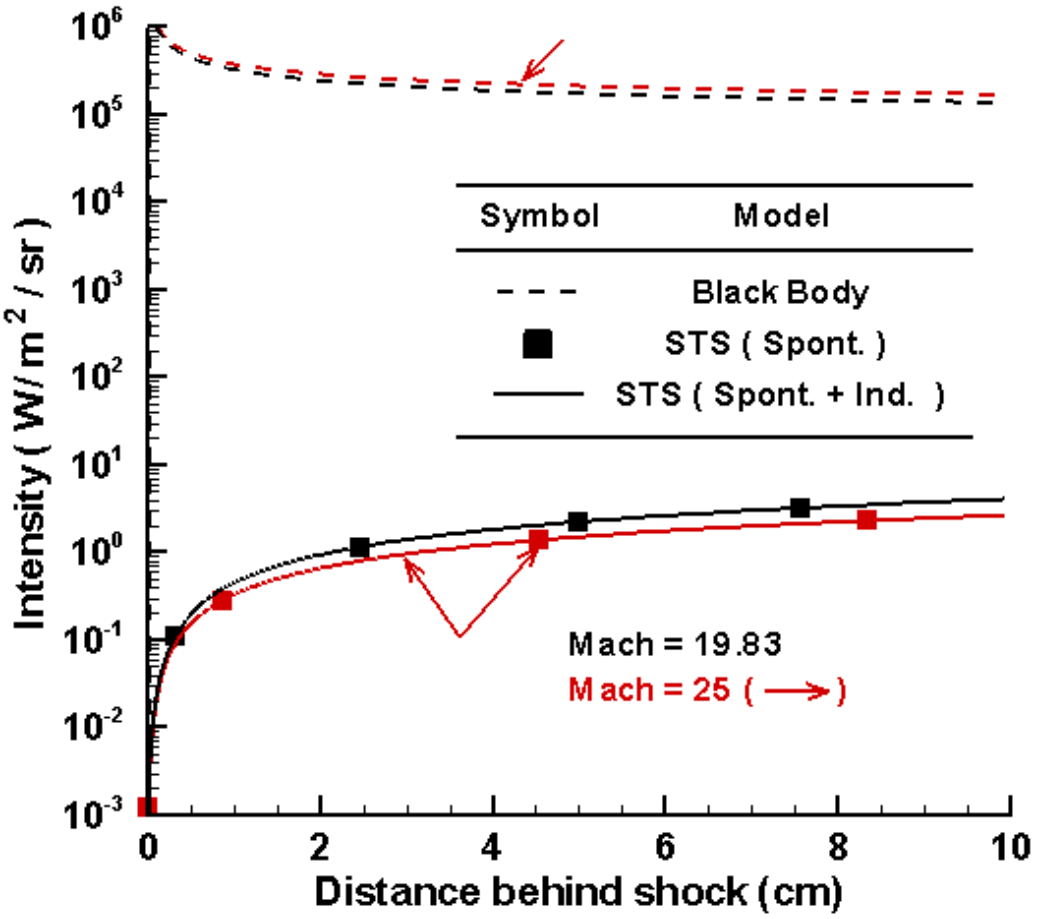

Fig.2. Radiation intensities behind the shock for different Mach numbers, obtained from black body and state-to-state (STS) approaches with/without the consideration of induced emission/absorption mechanisms.

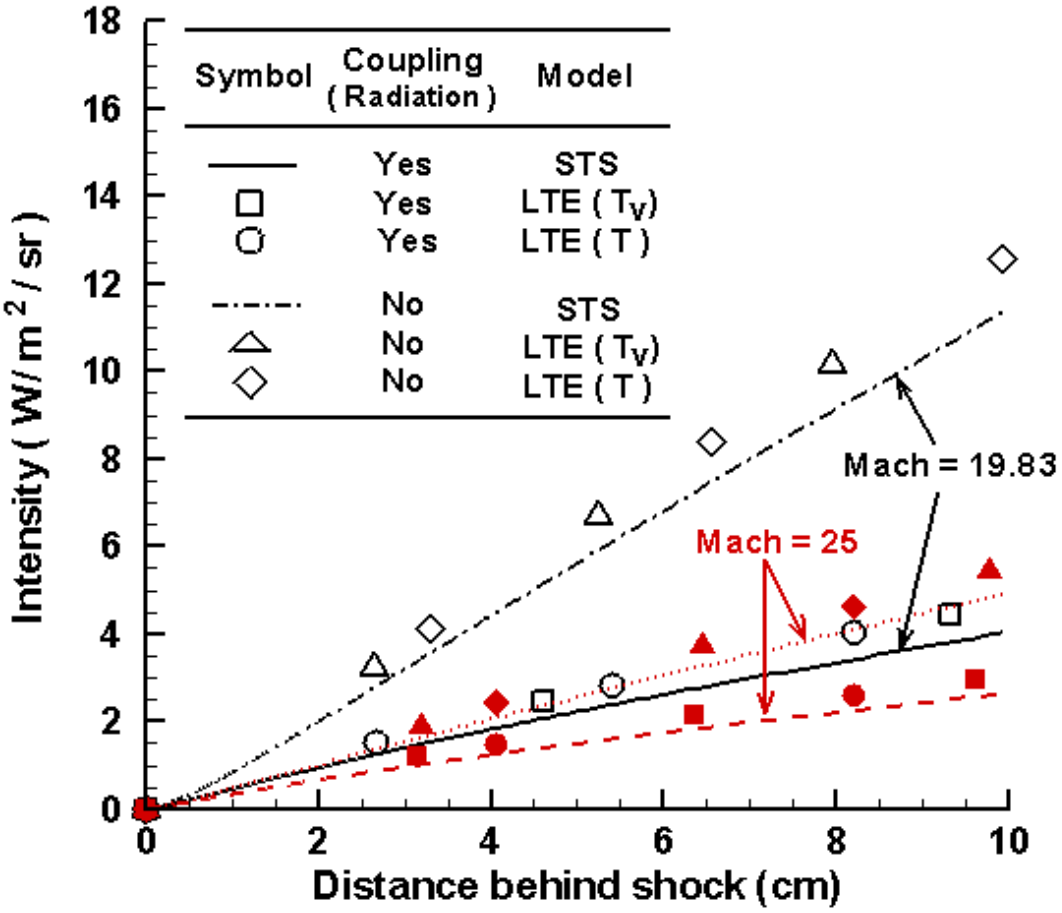

Fig.3. Radiation intensities behind the shock for different Mach numbers, obtained with and without the consideration of coupling between physicochemical and radiative processes based on STS and LTE (at T_v and T) approaches. Note that the unfilled and filled symbols correspond to Mach 19.83 and 25, respectively.

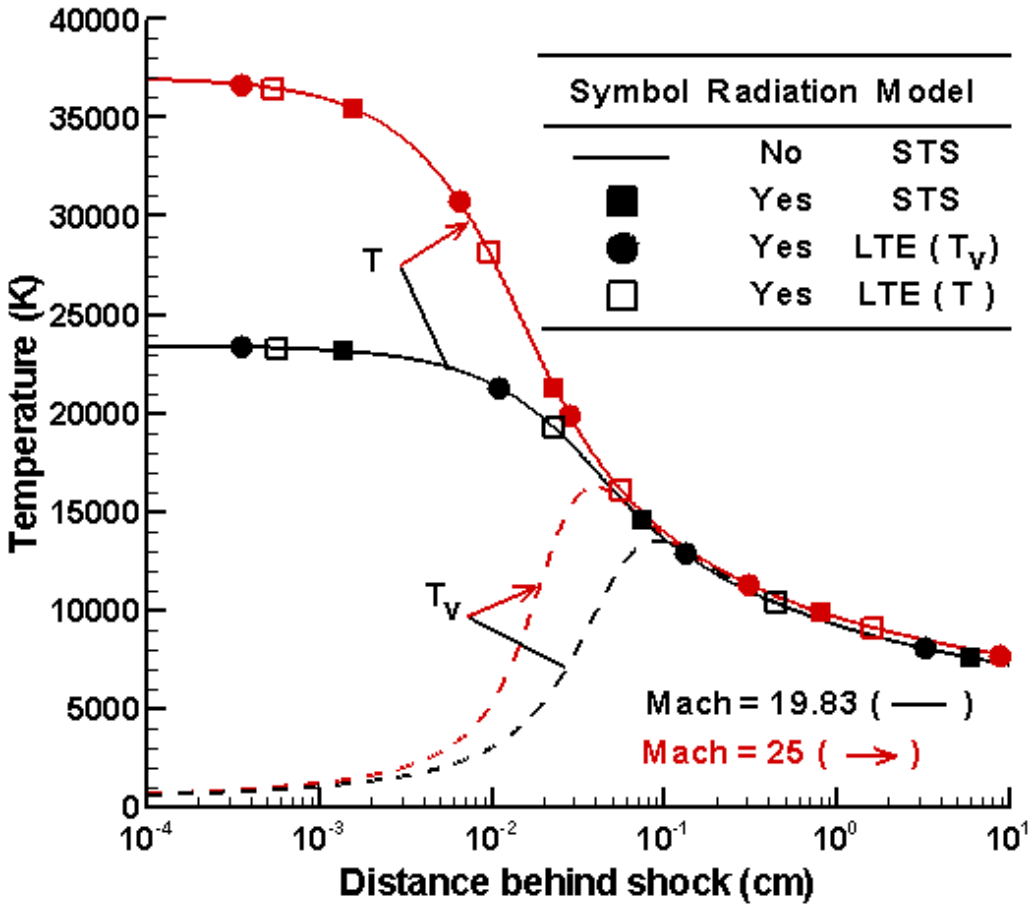

Fig.4. Rotational-translational and vibrational temperatures behind the shock with/without radiation based on STS and LTE at different Mach numbers.